Geochemical characteristics of the alkaline basalts and the phonolite –trachyte plugs of the Axum area, northern Ethiopia

Miruts HAGOS[1)*)], Christian KOEBERL[1)], Kurkura KABETO[2)] & Friedrich KOLLER[1)]

[1)] Department of Lithospheric Research, University of Vienna, Althanstrasse 14, A-1090 Vienna, Austria;

[2)] Department of Earth Sciences, Mekelle University, Mekelle, Ethiopia;

[*)] Corresponding author, miruts2005@yahoo.com

Abstract

The Axum volcanic rocks constitute important deposits of trap (Oligocene) and post-trap (Miocene- to Pliocene) volcanism at the northern end of the great Ethiopian flood basalt sequence. The petrologic diversity of lavas erupted in this area is significant, ranging from basanites to tephrites and phonolites to trachytes. The variation in the concentration of major elements (Fe_2O_3, TiO_2, CaO), rare earth elements (REE), and incompatible element ratios (Zr/Nb, Nb/Y) in the volcanic rocks of Axum demonstrates the heterogeneous character of their source region. Such heterogeneity can be interpreted by the involvement of a mantle reservoir to different degrees and mechanisms of partial melting. The geochemical data show that the Axum volcanic rocks represent two magma series, which we designate as the flood basalt sequence and the post-trap basalt sequence. The flood basalt sequence, which erupted contemporaneously with the Oligocene Ethiopian flood basalts, exhibit high TiO_2 (2.6 – 4.4 wt%), Fe_2O_3 (13.4 – 17.4 wt%), and high Zr/Nb ratio (9 – 18). In contrast, the post-trap basalt sequence, which has a slight tendency towards the composition of the north-central Ethiopian shield volcanoes (Guguftu shield volcano) and the central and southeastern Eritrean volcanic suites, exhibit low TiO_2 (2.0 – 2.6 wt%), Fe_2O_3(10.5 – 14.6 wt%), Zr/Nb ratio (2.8 – 3.1), and high Nb (60 – 84 ppm), Th (3.9 – 7.2 ppm), and Nb/Y ratio (2.2 – 2.7). The acidic rocks, on the other hand, are indistinguishable from each other and values of their trace element ratio are comparable with the trace element ratios of the post-trap basalt sequence. The acid volcanics (phonolites and trachytes) might, therefore, have formed mostly through fractional crystallization of the post-trap basalt sequence magmas.

Die am nördlichen Ende der großen äthiopischen Flutbasaltsequenz auftretenden Axum-Vulkanite bestehen aus Ablagerungen der oligozänen Trappvulkanite und den von Miozän bis Pliozän reichenden Posttrappvulkaniten. Die bedeutende petrologische Diversität der dort auftretenden Lava umfaßt Basanite bis Tephrite und Phonolite bis Trachyte. Der heterogene Charakter der Magmenquelle zeigt sich in der Konzentration der Hauptelemente (Fe_2O_3, TiO_2, CaO), dem Muster der Seltenerdelemente (REE) und in den Variationen der Verhältnisse einiger inkompatibler Elemente (Zr/Nb, Nb/Y). Solch eine Heterogenität kann durch Einfluß eines Mantelreservoirs mit unterschiedlichen Graden und Mechanismen einer partiellen Aufschmelzung interpretiert werden. Die geochemischen Daten zeigen, dass die Axum-Vulkanite zwei Magmaserien repräsentieren, die als Flutbasaltsequenz und Post-Trappbasaltsequenz bezeichnet werden können. Die Flutbasaltsequenz, welche gleichzeitig mit den oligozänen äthiopischen Flutbasalten austrat, zeigt hohe TiO_2 (2,6 – 4,4 wt%), Fe2O3 (13,4 – 17,4 wt%) und hohe Zr/Nb Verhältnisse (9 – 18). Die Posttrappbasalte andererseits, die in ihrer Zusammensetzung den nordzentralen Äthiopischen Schildvulkanen (Guguftu Schildvulkan) und den zentralen sowie südöstlichen Eriträischen Vulkaneinheiten ähneln, zeigen niedrige TiO_2 (2,0 – 2,6 wt%), Fe_2O_3 (10,5 – 14,6 wt%), Zr/Nb Verhältnisse (2,8 – 3,1), und hohe Nb (60 – 84 ppm), Th (3,9 – 7,2 ppm), und Nb/Y Verhältnisse (2,2 – 2,7). Die sauren Gesteine, andererseits, sind nicht voneinander zu unterscheiden. Die Verhältniswerte ihrer Spurenelemente sind mit denen der Posttrappbasaltsequenz vergleichbar. Die sauren Vulkanite (Phonolithe und Trachyte) dürften sich daher hauptsächlich durch fraktionierte Kristallisation aus dem Magma der post-Trappbasaltsequenz gebildet haben.

1. Introduction

The Axum study area is located in the northern part of the Ethiopian highlands and it is mainly covered by Tertiary flood basalts and the post-trap, east-west aligned Adwa-Axum phonolite and trachyte plugs (Hagos et al., 2010). These volcanic rocks were emplaced in the north - northwestern portion of the Tigray region, northern Ethiopia, isolated from the major Ethiopian flood basalts by the deeply cut Tekeze basin and from the Eritrean highland basalts and trachytes by the Mereb basin (Fig.1).

The Ethiopian volcanic province is one of the youngest flood basalt deposits on Earth and is a classic example to study young mantle plume processes underneath the Afar rift. This province is particularly favorable for the study of volcanism related to all stages of rift development (Barrat et al., 1998). Volcanism began in southern Ethiopia around 45 Ma (George et al., 1998), followed by flood basalt activity in northern Ethiopia and Yemen at ~30 Ma (Hofmann et al., 1997; Pik et al., 1999). Subsequent volcanism, from 22 Ma to present, occurs as large central vent volcanoes on the plateau or is associated with extension and localized in the rift axis (Pik et al., 1999). The Ethiopian landmass has experienced volcanic activities for a wide time span, from the Eocene to present. In northern

Ethiopia, in the Axum area, at least two phases of eruptive activity have taken place; the first during the Oligocene period ~30 Ma (part of the Ethiopian flood basalt) and the second during the Miocene – Pliocene periods (post trap basalts and phonolite/trachyte plugs).

The southern, central, and north-western part of the Ethiopian flood basalts have been the focus of numerous studies (e.g., Ayalew et al., 1999, 2002; Ebinger and Sleep, 1998; George et al., 1998; Kieffer et al., 2004; Mohr, 1983; Pik et al., 1998, 1999).

The existing studies in the Axum region (e.g., Alemu, 1998; Alene et al., 2000; Asrat et al., 2003, 2004; Tadesse, 1996, 1997) have mainly focused on the Precambrian basement and Pan African plutons of the area. The only study dealing with the volcanics of the Axum area was conducted during the regional mapping by the Ethiopian Institute of Geological Survey (1999). In this study,

FIGURE 1: Schematic map of the central, north-western and northern parts of the Ethiopian flood basalt province and the Afar triple junction with a box showing the location map of the Axum bimodal volcanics. The dividing line between high-Ti and low-Ti basalt province is marked by a dashed line (modified from Merla et al., 1979; Pik et al., 1998, and Kuster et al., 2005). CFB = continental flood basalts.

the volcanic rocks of Axum were classified on the basis of the locality names as the Koyetsa volcanic (stratified flood basalt) and the Adwa trachyte formation (trachytic and phonolitic plugs). However, detailed geological investigations are still rare in the Axum region. Petrologic and geochemical classifications of the area were made based on analyses of samples collected from the Mai-chew area and of northwestern flood basalts. As a result of limited sampling the geological classifications were not representing the actual volcanic rocks of the Axum area.

In this study we have focused on the geochemical (major and trace element) characteristics of the Axum phonolites and trachytes in relation to the alkali basalts (Hagos et al., 2010), and possible petrogenetic relationships among them. We have also compared the spatial and temporal variation of the Axum volcanic rocks with the central–northwestern Ethiopian shield volcanoes and the central–southeastern parts of the Eritrean volcanic rocks.

2. Geological background

Most continental flood basalts are associated with lithospheric extensions resulting from distant and/or local stress fields. The Ethiopian volcanic province is one of the youngest flood basalt provinces, and is related to the opening of the Red Sea and the Gulf of Aden (Baker et al., 1996; George et al., 1998). The flood basalts were unconformably emplaced on a regionally lateritized sandstone surface (Ukstins et al., 2002) and some on deeply eroded basement complexes. Lavas of this province
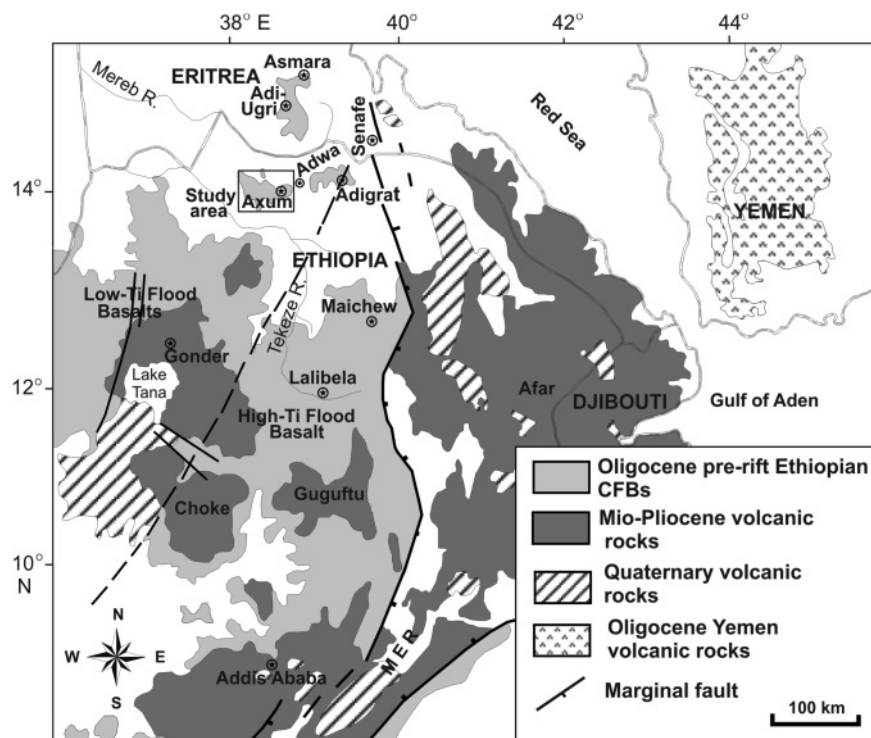
erupted 30 Myr ago, during a short 1 – 2 Myr period, to form a vast volcanic plateau (Baker et al., 1996; Hofmann et al., 1997). However, rift-triggered magmatism with an age range of 14 – 5 Myr and pre-rift, lower Oligocene (Stewart and Rogers, 1996) volcanic rocks are common to the east and south of the main Ethiopian flood basalt respectively. The basalts are partly overlain by relatively younger rhyolitic/trachytic and phonolitic volcanoes (Ayalew et al., 1999).

The mineralogical and chemical composition of the flood basalt is relatively uniform and most rocks are aphyric to sparsely phyric, and contain plagioclase and clinopyroxene phenocrysts with or without olivine (Kieffer et al., 2004). Despite their compositional similarities, the Tertiary flood basalts of Ethiopia were divided into three types based on their temporal variations (Mohr, 1983). In ascending stratigraphic order, these are called the Ashange, Aiba, and Alage basalts. In contrast to the above classification, based on geochemistry Pik et al. (1998, 1999) divided the Ethiopian flood basalts into three distinct magma types: low-Ti basalts (LT), high-Ti 1 basalts (HT1), and high-Ti 2 basalts (HT2) (Fig.1). These authors recognized a suite of 'low-Ti' basalts (LT) characterized by relatively flat chondrite-normalized rare earth element (REE) patterns and low levels of Ti and incompatible trace element contents. According to these authors, the HT2 basalts have high levels of Ti and incompatible elements and show extreme fractionation of the REE, whereas the HT1 basalts exhibit intermediate characteristics between LT and HT2.

Inter-fingering with the flood basalt, particularly at upper stra-

tigraphic levels, are felsic lavas and pyroclastic rocks of rhy- olitic, or, less commonly, trachytic compositions (Ayalew et al., 1999, Kabeto et al., 2004, Zanettin et al., 2006b). The volume and aerial coverage of these felsic rocks substantially increase towards the northern end (Tigray and Eritrea) of the Ethiopian volcanic province. The trachytes occur as plugs (steep-sided conical hills), and lie within an E – W belt extending from the eastern margin of the Ethiopian plateau, between Adigrat and Senafe, via Adwa and Axum, westward to the middle Tekeze river valley. There, the trachytic domes reach their maximum frequency and dimension and lie indistinguishably on the Ara- bian-Nubian shield, Mesozoic sandstone, and Oligocene vol- canic rocks of the region (Zanettin et al., 2006b).

The felsic rocks of Axum-Adwa area and, by analogy, those of the Senafe domes (southeastern Eritrea) were coeval with the rhyolitic layers intercalated with the stratoid basalt (traps) occurring in both Tigray and in the central Eritrean plateau (Dainelli, 1943). The geochemical data show that the felsic rocks of the region are highly diversified, ranging from the rhy- olite field to the phonolitic tephrites (Zanettin et al., 2006). Ac- cording to these authors, the dykes and domes occurring in the Adwa-Axum and Senafe area belong to different magmatic series: transitional, mildly alkaline, and strongly alkaline.

3. Geology and petrography of the Axum volcanic rocks

The Axum volcanic rocks constitute an important outcrop of trap basalts and post-trap basalts as well as phonolite – tra- chyte plugs at the northern end of the Ethiopian flood basalt province. They are about 5 – 500-m-thick sequences exposed around the Axum and Shire regions, covering a total area of about 1200 km². The Axum volcanics are visually classified into the Axum basaltic sequences and the phonolite – trachyte plugs.

3.1 The Axum basaltic sequences

In the study area, the Mesozoic sedimentary rocks and/or basement complexes are unconformably overlain by the Ethio- pian Plateau flood basalts erupted between 31 - 29 Ma (Hof- mann et al., 1997) and the later phase basaltic rocks. Based on field observations and mineralogy, these volcanic rocks are broadly subdivided into two major sequences. These are the post-trap basalt sequence and the flood basalt sequence.

Post-trap basalt sequence: this sequence is located about 5 -10 km south of the town of Axum, mainly unconformably over- lying the sheared, deformed and deeply weathered basement complex of Deigo and Adi-Tsehafi villages at an altitude of 2020-2130 m. The rocks are gently inclined (<5°), 5 – 60 m thick, and show southwest lava flow direction. They are rarely vesicular, columnar jointing, and commonly less weathered than the adjacent flood basalt sequence. The lava flows of this basaltic sequence are thicker but less continuous than the neighboring flood basalt sequence. Normally, such rocks are laterally discontinuous and usually exposed along the deep canyons of the southern and northern part of the area (Fig. 3).

The basalts are commonly aphyric to highly phyric with a significant amount of phenocrysts (Fig. 2a). The phenocryst minerals constitute about 25 vol% and comprise euhedral to subhedral pyroxene, olivine, and plagioclase-lath. More over opaque minerals (ilmenite, magnetite) constitute up to 20 vol% in the matrix. The groundmass is dominated by plagioclase and pyroxene.

Flood basalt sequence: this sequence, about 350 – 400 m thick and commonly exposed in the central and western part of the area at an altitude between 2080 – 2600 m, is invaria- bly weathered and intercalated with thin pyroclastic (ash-tuff fallout) materials. This basaltic sequence, unconformably over- lying the clastic Mesozoic sedimentary rocks of the region, is the western extension of the Adigrat basaltic sequence, but is isolated from the Adigrat basalts by the Adwa basin. The ve- siculated and weathered parts of this sequence contain some secondary minerals like calcite veins in addition to silica and zeolites. These rocks show extensive aerial distribution and erosion formed domical edifices that rise to about 300 m – the Ferasit and Morer ridges. These volcanic rocks comprise coarse-grained, plagioclase-phyric, ± K-feldspar-bearing ba- salts. The feldspars are well aligned and show well-preserved flow texture. In most of the samples, the pyroxenes exist as euhedral to subhedral mega-phenocrysts (Fig. 2b).

3.2 Miocene- to Pliocene-age Axum Phono- lite – Trachyte plugs

Widespread volcanic to hypabyssal igneous materials, for- ming steep sloped plugs and ridges, were produced probably between 7 and 3 Ma (Beyth, 1972), when they punctured and partially extruded/intruded the upper part of the clastic Meso- zoic sedimentary and the Tertiary flood basalt sequence. These, silica-poor volcanic to hypabyssal rocks belong to the Axum- Adwa phonolite–trachyte volcanic field and are exposed mostly at the north side of the study area (Fig. 3). The variation in mineralogy is gradational and ranges from nepheline-rich pho- nolite (Bete-Giorgis phonolites)- to nepheline-poor phonolitic- trachyte (Adi-Tsehafi trachytes) and trachytes (Mai-Koho tra- chytes).

3.2.1 Bete-Giorgis Phonolites

These rocks are emplaced directly at the northwestern end of the town of Axum and about 4 km to the northeast of the Gobo-Dura ridge. The exposure is in the form of a large, com- pletely exposed, circular (~3.2 km in diameter) erosional dome rising about 300 m above the alkaline basalts. Only few pri- mary structures and secondary features such as some colum- nar joints along the hilly parts of the dome and weak sphero- idal-type weathering in some of the rounded blocks are ob- served in the dome. The phonolitic rocks are still massive, but moderate weathering along fracture surfaces and complete alteration along contacts and weak zones occur. The Bete- Giorgis phonolite plugs show a zoned texture with a light co- lored and fine-grained rim at the contact with the trachytes, and a dark-colored, medium- to coarse-grained core. The up-

hill part of the dome is relatively flat and covered by debris of the fine-grained phonolites.

The Bete-Giorgis phonolites have variable texture. They are porphyritic with phenocrysts of alkali pyroxene, nepheline, and feldspars. Under plane polarized light, the pyroxenes have high-relief, brownish- to greenish color, with needle-like to skeletal form. The nephelines are rectangular- to hexagonal in shape and some exist in the form of inclusion inside the alkali pyroxene phenocrysts (Fig. 2c). In some of the samples (AX 43 and AX111) the nephelines are highly altered to zeolites and they mask the presence of other minerals. The aegirines are tabular- to elongated and in places they grew at the rims of other minerals.

3.2.2 Gobo-Dura phonolites

Five km west of Axum, along the road to Shire, there is an about 200 – 250 m thick, circular (3.5 km in diameter) and dome-shaped phonolite outcrops. They are dark-gray to pink in color, extremely massive, unweathered, and occur in places as 35-m-long single blocks. Most of the blocks are tabular and elongated, but few form spherical outcrops. Despite its unique lithologic setup the Gobo-Dura ridge constitutes various relics reflecting the ancient architecture of the Axumite Empire. At the northeastern part of the dome, there is ancient, (~1700 years old) quarry-site hosting dozens of semi-finished obelisks. To further study the mineralogical and geochemical characteristics of these archaeologically important rocks, five

samples were collected for analyses.

Petrographically, the Gobo-Dura phonolites are also dominated by phenocrysts of pyroxene, nepheline, and some early crystallized sanidine. The pyroxenes are light-brown to green with distinct relief under plane polarized light. Very large grains of partly altered, subhedral to anhedral nephelines mask other low-relief minerals (Fig. 2d). Highly altered mafic minerals and some intergrowths of aegirines surround the nepheline phenocrysts. Tightly locked needle-like feldspars filled the interstices of the pyroxenes.

3.2.3 Adi-Tsehafi trachyte

About five km to the north of the town of Axum, where the river Gwada turns to the north, the great unconformity that separates the late-Proterozoic granitic intrusion and the clastic Mesozoic sedimentary rocks is injected by the Miocene- to Pliocene rocks of the area. These are subvolcanic bodies (sills) exposed along the Gwada river after intense erosion of the overlying rocks (sandstone and trap basalts). These sills are about 15 m thick, and comprise massive, partially weathered and fine- to medium-grained rocks. The second-largest quarry-site, which was in operation during the time of King Kaleb (~520 AD) of the Axumite Empire, is situated at this outcrop. The length of a single block of rock does not exceed 15 m, but this quarry site was mainly used as a source for rocks used for inscriptions and various underground and gravestone works during the reign of King Kaleb. To study the geochemi-
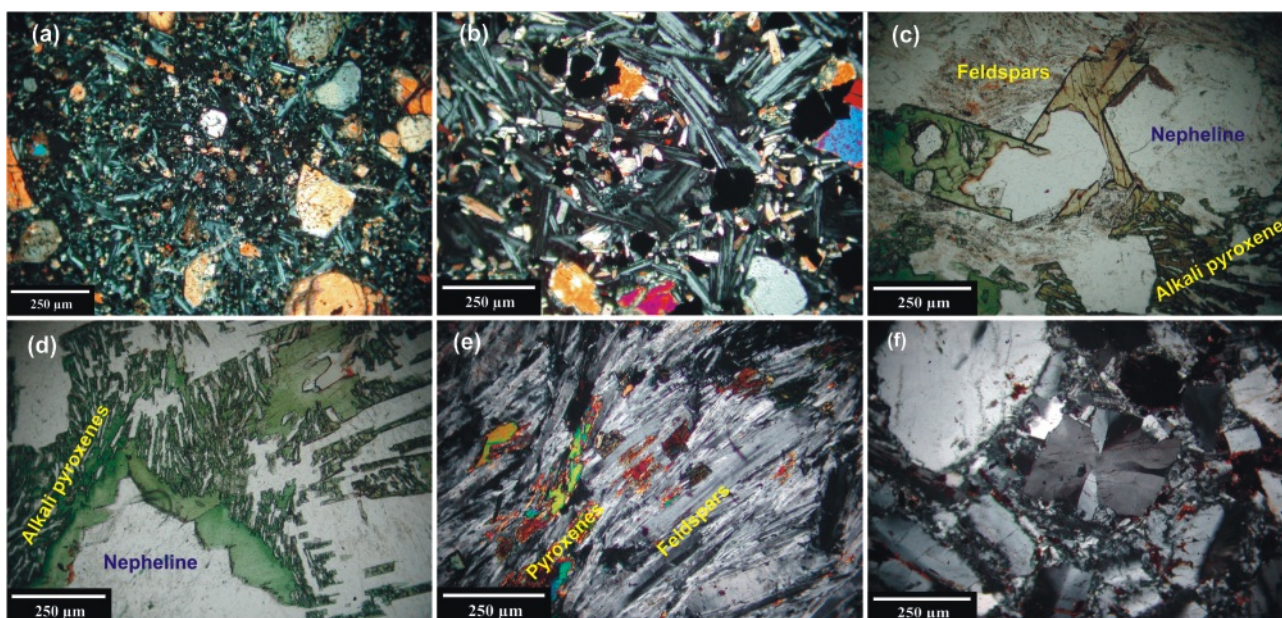

Figure 2: Petrography of the volcanic rocks of Axum area showing various mineralogical and textural features. Images (a), (b), (e) and (f) were taken under crossed polarizers, whereas (c) and (d) were taken under plane polarized light. (a) Aphyric–phyric, plagioclase rich alkali basalts with medium - coarse-grained phenocrysts of olivines and clinopyroxenes; the plagioclase are lath-like but randomly aligned, where as the phenocrysts are rounded to angular of varying size. (b) Coarse-grained, plagioclase-phyric, ± K-feldspar bearing basalts. Dark-colored minerals of Ti oxides and Mg oxides are filling the interstices of other grains. (c) Highly porphyritic with phenocrysts of alkali pyroxene, nepheline, sodic pyroxene/aegerine and feldspars. (d) Phenocrysts of pyroxene, nepheline, sodic pyroxene, and some early crystallized feldspars. Highly altered mafic minerals and some intergrowths of aegirines surround the nepheline phenocrysts. (e) Dark-colored, well aligned, elongated- to needle-like, tightly packed grains of K-feldspar with few anhedrally shaped nephelines. This sample is transitional between trachytes and phonolites (Gobo-Dura phonolites). (f) Fine- to coarse-grained (inequigranular) elongated and in some cases euhedral-shaped K-feldspars with well-developed trachytic textures are the main constituents. Most of the phenocrysts show simple twinning and others spherulitic texture.

cal characteristics of these rocks, three samples were analyzed for their major and trace element contents. The Adi-Tsehafi trachytes constitute needle-like- to elongated, holocrystalline, medium-grained feldspars (orthoclase) and sparsely distributed dark-green sodic pyroxenes/aegirines. Most of the minerals are highly weathered but some subhedral- to anhedral nepheline crystals filled the interstices of the feldspars (Fig. 2e).

3.2.4 Mai-Koho trachytes

At the northern and northwestern part of Axum, trachyte flows cut by phonolite plugs are widely distributed and at places they formed mountain-chains as high as 500 m. They are considered to be the western extension of the Senafe–Adwa trachytic plugs (Zanettin et al., 2006b), but with a remarkable shift in their morphology. The Senafe–Adwa trachytic plugs are steeper and taller (~1000 m) than the Axum trachytic plugs, which are dome-shaped and not >400 – 500 m tall. The Mai-Koho trachytes are whitish-grey in color, soft, moderately weathered, thinly layered and intensely fractured. These rocks are

commonly emplaced adjacent to the phonolites, but they are steep plugs and form chain-like exposures.

Fine- to coarse-grained (inequigranular) elongated and in some cases euhedral K-feldspars with well developed trachytic textures are the main constituents of the outcrop. The feldspars occur both as groundmass and as phenocrysts. Some of the phenocrysts show simple twinning and others have spherulitic texture. Some mafics (dark minerals) exist, but they are highly oxidized (Fig. 2f).

4. Geochemical Data

4.1 Sampling and Analytical methods

Our sampling set out to include both the mafic and felsic volcanic rocks of Axum. Thirty-three samples were carefully selected from 112 samples collected from the entire Axum area and prepared for X-Ray Fluorescence (XRF) spectrometry and Instrumental Neutron Activation Analysis (INAA). 100-200 g of clean, unaltered interior chips were selected from approxi-
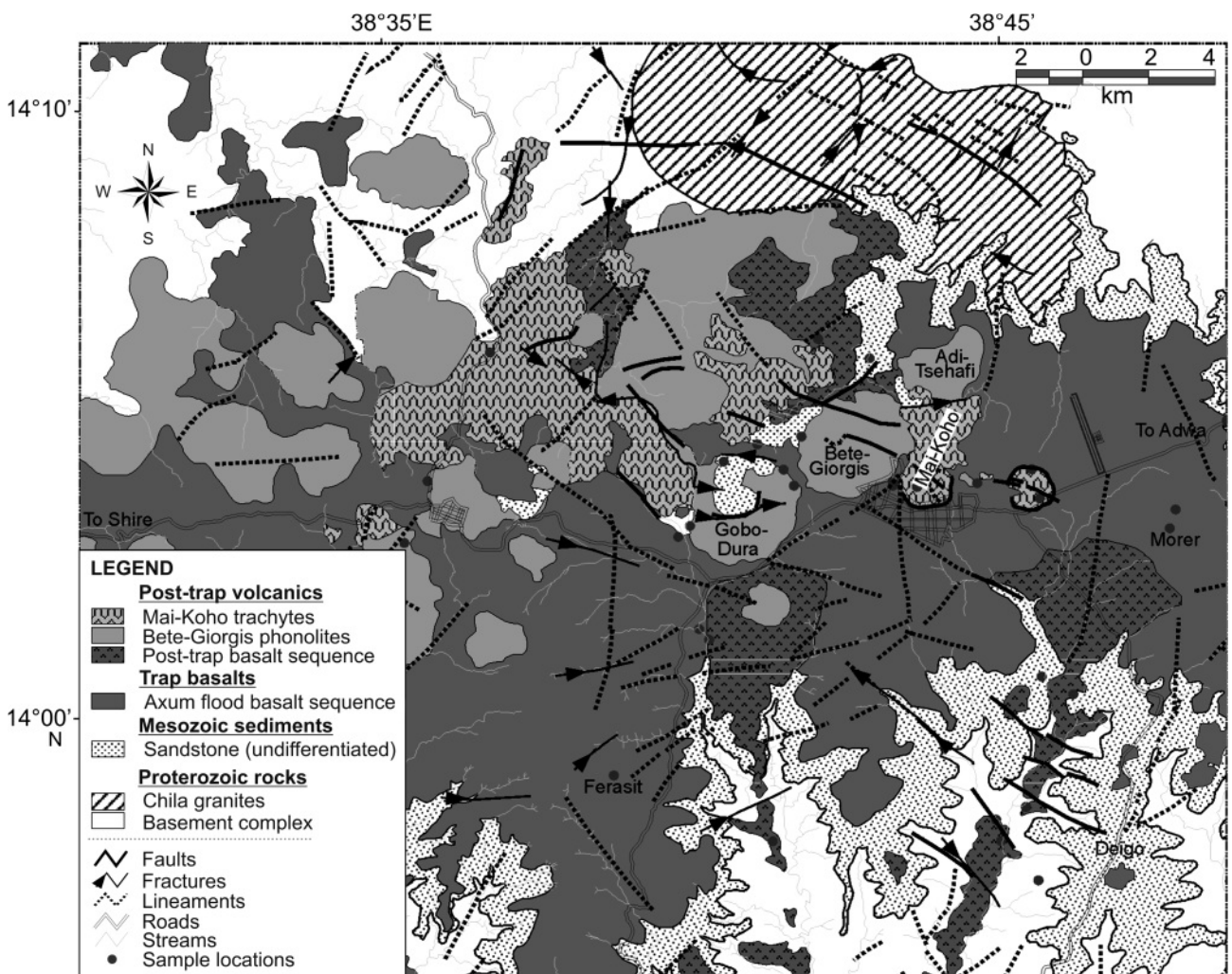
Figure 3: Geological map of the volcanic rocks of Axum area. The 1:50,000 scale topographic maps of Axum, Adwa, Enda-Silasie, and Chila were taken as a base map. The spatial variations of rocks, lithologic contacts, and the structures were extracted from 1:50,000 scale aerial photographs (Eth94), Landsat ETM+ 2002, and ASTER. Color composite images of Landsat bands 7, 5, and 2 are commonly used to differentiate between the clastic Mesozoic sedimentary rocks and the overlaying flood basalts, but geologic structures such as faults, fractures and lineaments were extracted from aerial photographs (ETH94). In some areas the high spatial resolution image, the ASTER image was used (modified from Hagos et al., 2010).

	Trachyte AX002	Trachyte AX008	Phonolite AX011	Phonolite AX012	Trachyte AX41	Phonolite AX43	Phonolite AX45	Phonolite AX45c	Trachyte AX51	Phonolite AX111	Phonolite AX112	Phonolite AX06	Trachyte AX07	Phonolite AX10a	Trachyte AX10b
(wt.%) SiO_2	66.65	68.61	62.32	62.21	62.81	59.28	62.03	62.41	65.53	58.82	58.62	61.92	62.53	61.80	62.35
TiO_2	0.15	0.03	0.04	0.06	0.06	0.03	0.04	0.06	0.15	0.03	0.03	0.05	0.08	0.06	0.09
Al_2O_3	16.52	16.78	17.83	17.84	17.84	18.97	17.84	17.93	17.40	18.81	18.55	17.35	16.82	17.36	16.70
Fe_2O_3	4.19	2.83	4.82	5.14	4.39	5.44	4.87	4.87	4.26	5.51	5.46	5.19	5.83	5.57	5.92
MnO	0.14	0.18	0.24	0.21	0.21	0.30	0.24	0.21	0.14	0.30	0.29	0.22	0.22	0.22	0.24
MgO	0.01	0.01	0.01	0.01	0.01	0.01	0.01	0.01	0.01	0.14	0.01	0.10	0.19	0.08	0.10
CaO	0.64	0.40	0.66	0.88	0.65	0.99	0.60	0.84	0.14	1.50	0.87	0.89	0.79	0.97	1.21
Na_2O	6.60	6.62	9.23	8.57	8.58	9.77	9.60	8.58	6.57	8.85	9.88	7.71	7.57	7.89	7.27
K_2O	5.10	4.93	4.82	5.09	4.74	4.89	4.82	5.14	5.38	5.12	4.82	5.70	5.26	5.51	5.33
P_2O_5	0.02	0.03	0.03	0.04	0.03	0.04	0.03	0.04	0.05	0.03	0.04	0.02	0.02	0.02	0.02
LOI	1.01	0.76	0.83	1.05	1.79	1.07	0.84	0.88	1.16	1.94	2.13	3.04	2.65	4.97	3.50
Total	101.03	101.18	100.83	101.1	101.11	100.79	100.92	100.97	100.79	101.05	100.70	102.20	101.94	104.44	102.74
(ppm)															
Sc	1.34	0.76	0.97	0.87	0.74	0.83	0.86	0.67	1.23	0.86	0.88	--	--	--	--
V	38	41	38	38	39	38.0	39	38	43	30	38	1	6	3	2
Cr	8.23	9.49	10.3	8.85	6.09	8.30	8.68	5.64	6.77	9.41	9.08	<0.01	5.1	2.14	<0.01
Co	0.35	0.24	<0.04	0.47	0.34	0.23	0.2	0.35	1.96	0.18	0.38	--	--	--	--
Ni	15	8	17	12	15	14	18	17	24	18	16	202	252	192	260
Cu	<2	<2	<2	<2	<2	<2	<2	<2	<2	<2	<2	--	--	--	--
Zn	209	153	250	182	204	264	272	198	190	278	285	--	--	--	--
Ga	41	29	48	42	42	42	49	52	45	52	54	39	51	38	51
As	3.93	1.9	6.59	4.18	3.9	2.66	5.71	4.99	4.57	3.65	6.76	--	--	--	--
Se	1.93	2.31	4.31	0.31	0.31	1.16	0.20	<2.6	<2.1	0.88	1.48	--	--	--	--
Br	<1.1	<1	2.91	2.21	<6.2	8.92	6.73	3.60	<5.2	<2.8	5.74	--	--	--	--
Rb	235	208	321	232	264	283	350	249	277	285	290	239	298	237	293
Sr	13	23	9	3	6	3	<2	49	10	17	3	7.84	1.77	3.48	55.4
Y	94	47	113	83	92	152	115	113	91	120	122	79	114	71.0	127
Zr	471	295	908	707	1236	1079	944	817	935	846	853	1148	1449	1042	1552
Sb	0.23	0.17	0.56	0.34	0.20	0.19	0.34	0.24	11.2	0.93	0.44	--	--	--	--
Nb	206	128	237	195	249	290	241	229	231	243	251	202	252	192	260
Cs	1.30	2.01	4.00	2.91	2.82	3.46	4.25	2.58	2.27	3.83	4.05	--	--	--	--
Ba	47.6	92.7	30.1	20.7	25.4	26.4	39.5	23.6	51.8	32.3	32.3	16.2	20.3	19.9	21.1
La	144	75.1	183	134	160	171	194	142	129	203	195	--	--	--	--
Ce	282	142	346	240	270	323	352	255	275	338	352	358	433	326	443
Nd	103	44.5	119	97.9	89.1	121.1	127	95.9	76.8	132	132	--	--	--	--
Sm	17.5	7.89	22.4	18.3	17.1	23.7	24.9	19.1	16	28.1	26.2	--	--	--	--
Eu	1.16	0.82	1.72	1.41	0.87	2.19	1.69	1.43	0.63	2.33	2.32	--	--	--	--
Gd	15.6	5.82	26.8	16.0	16.9	19.9	22.9	19.6	15.6	23.0	25.5	--	--	--	--
Tb	2.73	1.16	3.6	2.52	2.27	3.37	3.53	2.77	2.56	3.65	3.71	--	--	--	--
Tm	1.69	0.83	2.24	1.62	1.85	2.02	2.28	1.63	1.77	2.11	2.19	--	--	--	--
Yb	9.49	5.43	12.1	8.51	8.92	10.8	12.2	9.73	10.3	12.4	12.2	--	--	--	--
Lu	1.47	0.85	1.77	1.28	1.32	1.59	1.80	1.38	1.51	1.69	1.73	--	--	--	--
Hf	19.5	14.1	32.6	23.7	40.0	31.7	35.2	27.4	34.8	33.3	30.1	--	--	--	--
Ta	15.3	14.3	20.9	16.3	20	20.85	23.5	15.7	17.8	22.0	22.3	--	--	--	--
W	3.71	1.49	1.28	5.56	<6.2	3.51	3.5	<4.5	1.65	5.75	2.62	--	--	--	--
Ir (ppb)	<1.1	<1	3.04	<1.1	<1.8	<1.6	<1.7	<2	<1.7	<1.7	<1.8	--	--	--	--
Au (ppb)	<1.7	<1.7	<2	<1.2	<2	<2.3	<3.2	<2.2	<2.5	<0.01	<2.7	--	--	--	--
Th	28.1	21.5	39.2	19.6	32.1	27.3	38.0	26.7	30.4	31.9	33.9	24.6	24.1	21.7	26.5
U	4.74	4.56	8.79	6.66	7.11	9.13	10.7	7.76	6.6	12.1	9.77				
(Eu/Eu*)n	0.21	0.33	0.21	0.25	0.17	0.30	0.22	0.23	0.12	0.28	0.27				

	Basalt AX004	Basalt AX08	Basalt AX20	Basalt AX21	Basalt AX24	Basalt AX29	Basalt AX31	Basalt AX32	Basalt AX34	Basalt AX38	Basalt AX42	Basalt AX43d	Basalt AX44	Basalt AX46	Basalt AX47b	Basalt AX63	Basalt AX79	Basalt AX09
(wt.%) SiO_2	43.05	54.37	43.63	44.06	49.20	48.32	48.19	46.82	48.65	44.32	50.68	48.76	47.06	51.60	45.75	44.82	50.96	45.13
TiO_2	4.39	1.85	2.56	2.95	2.10	3.50	2.12	3.25	2.25	2.44	2.90	2.23	2.85	1.54	2.17	3.07	1.58	3.97
Al_2O_3	13.88	15.67	15.49	14.85	15.87	15.32	19.22	16.51	15.93	15.58	16.24	16.67	16.38	16.92	14.57	14.32	16.68	15.16
Fe_2O_3	17.32	9.71	12.94	12.85	10.82	15.39	10.85	14.89	11.12	11.64	13.42	14.57	15.84	12.55	11.68	16.26	12.61	16.58
MnO	0.21	0.17	0.22	0.20	0.19	0.20	0.21	0.17	0.20	0.20	0.19	0.15	0.14	0.24	0.20	0.24	0.25	0.18
MgO	7.22	2.01	7.73	7.89	7.68	4.60	3.32	5.22	7.92	6.82	3.63	3.84	3.52	2.45	11.02	5.66	2.64	5.44
CaO	7.90	5.46	10.59	9.90	9.42	7.08	7.90	6.87	9.35	11.69	7.22	5.16	4.71	4.93	10.72	7.68	5.48	7.07
Na_2O	4.17	4.01	4.13	4.36	3.96	3.87	5.30	3.86	3.69	4.28	3.35	6.19	5.94	6.87	2.85	5.34	6.38	3.46
K_2O	1.59	2.97	1.71	1.12	1.93	1.05	2.08	1.12	1.84	1.04	1.74	0.96	0.58	1.50	1.53	1.47	1.54	1.37
P_2O_5	0.96	0.66	0.69	0.76	0.55	0.53	0.80	0.48	0.53	0.84	0.80	0.67	0.59	1.51	0.57	1.30	1.53	0.60
LOI	0.72	4.13	1.93	2.81	0.17	1.89	1.41	1.53	0.24	2.57	1.18	2.29	3.08	0.91	0.63	1.05	1.44	2.88
Total	101.41	101.01	101.62	101.75	101.89	101.75	101.40	100.72	101.72	101.42	101.35	101.49	100.69	101.02	101.69	101.21	101.09	101.83
(ppm)																		
Sc	13.7	15.4	22.3	18.2	17.7	19.2	6.7	20.6	21.9	24.3	19.5	6.81	6.14	5.42	24	10.9	5.42	
V	199	126	254	227	201	207	142	266	212	240	225	79	76	48	242	139	47	384
Cr	14.9	17	106	128	273	11.0	9.7	39.3	386	226	23.6	97.1	28.7	9.06	579	8	7.06	39.5
Co	44.2	17.9	40.9	33.5	31.9	35.5	20.7	52.0	43.9	40.7	34.6	31.9	38.5	14.3	49.9	32.0	14.3	--
Ni	34	14	71	90	143	22	5	52	161	112	27	17	46	10	245	12	8	18.6
Cu	25	17	6	41	66	29	6	30	57	70	36	13	19	2	73	9	4	--
Zn	165	137	115	97.8	99.0	140	90.4	165	124	112	171	132	136	155	115	192	150	--
Ga	29	22	16	18	18	24	16	24	18	16	22	21	22	25	16	32	25	24
As	1.04	0.18	<1.5	1.71	0.45	<1.5	0.45	<1.5	<2.1	<2.3	0.32	<3.2	<1.5	1.36	0.48	1.17	<1.9	--
Se	<1.7	<1.64	0.26	2.19	2.19	<2.9	<2.2	3.05	<3.1	<2.4	<2.8	<2.5	<2.3	<2.5	<3.8	<2.8	<2.5	--
Br	<0.7	<0.75	<1	1.50	1.37	<3.86	1.91	<3.9	<4.9	<5.2	<3.5	<5.3	<4	<5.1	<3	<5.1	<4.4	--
Rb	41.0	37.4	64.7	35.9	36.7	12.3	48.3	19.6	41.7	16.1	51.8	26.7	16.2	25.1	30.0	21.3	29.5	17.7
Sr	989	559	786	983	796	619	1163	680	737	927	760	704	1020	1776	789	1207	1760	614
Y	30	44	31	34	28	39	29	36	28	31	45	16	23	61	27	36	62	37
Zr	321	389	192	258	197	212	222	208	190	211	269	209	315	637	173	389	621	267
Sb	0.10	<0.14	0.09	0.04	0.02	<0.13	0.07	<0.2	0.21	0.10	0.09	<0.1	<0.2	<0.2	<0.1	0.85	0.14	--
Nb	34	23	69	84	70	12	77	15	65	73	20	10	20	37	60	40	35	19
Cs	0.42	0.34	0.64	0.54	0.26	<0.2	0.89	0.36	0.43	0.74	0.61	0.22	3.18	0.91	0.33	0.48	0.38	--
Ba	110	640	523	378	363	221	433	270	431	664	460	178	65.4	176	453	116	150	504
La	30.4	38.3	46.8	60.8	47.4	15.2	55.5	20	47.4	55.9	31.1	20.9	15.1	42.7	41.1	38.4	41.1	--
Ce	72.6	84.2	86.1	110	80.8	38.2	102	47.4	86.5	98.2	72.0	53.6	44.8	108	71.7	90.3	104	47.3
Nd	46.8	45.2	31.5	45.9	32.5	27	42.3	30.6	34.8	44.3	42.1	38.7	38.5	70.8	35.8	56.9	68.4	--
Sm	11.3	9.91	7.29	8.86	6.33	7.27	7.91	8.38	7.62	8.80	10.4	10.3	10.6	17.3	7.24	14.3	16.6	--
Eu	4.25	3.79	2.46	3.02	2.24	2.62	2.70	2.85	2.44	2.70	3.27	3.37	3.49	5.73	2.35	4.59	5.66	--
Gd	9	9.13	6.76	7.69	6.18	9.20	9.07	10.2	9.52	9.81	11.2	9.07	12.4	19.4	8.82	15.1	15.6	--
Tb	1.46	1.43	1.07	0.93	0.84	1.16	1.03	1.39	1.03	1.08	1.56	1.22	1.33	2.26	0.86	1.71	2.18	--
Tm	0.37	0.68	0.59	0.56	0.47	0.67	0.73	0.75	0.7	0.67	0.82	0.38	0.36	1.08	0.59	0.54	1.08	--
Yb	1.80	3.93	2.57	2.69	2.18	2.81	2.63	2.85	2.37	2.76	3.63	1.34	1.37	5.18	2.23	2.03	4.89	--
Lu	0.22	0.62	0.37	0.38	0.31	0.43	0.38	0.45	0.32	0.4	0.54	0.15	0.17	0.75	0.32	0.24	0.70	--
Hf	8.63	10.6	4.16	5.81	4.02	5.23	4.67	6.08	4.49	4.63	7.33	8.27	8.04	17.0	3.52	10.3	16.7	--
Ta	2.51	1.33	4.97	5.55	4.53	0.62	5.61	1.13	4.90	4.67	1.32	1.36	1.00	3.12	4.07	2.84	2.86	--
W	3.10	<3.42	<4.39	0.41	0.38	<2.4	0.15	<2	<3.6	<4.1	<2.1	2.14	<2.2	<3.6	<1.7	<3.5	<3	--
Ir (ppb)	<1.6	<1.6	<1.4	2.99	3.05	<2.4	<1.7	<2.6	<2.9	<2.1	<2.3	<2.2	<1.9	<2	<3.2	<2.3	<2	--
Au (ppb)	2.02	0.98	0.8	0.82	0.78	<2.1	1.1	<2.2	<2.3	<0.01	<0.01	<0.01	<2.3	<0.01	<1.8	<2.5	<0.01	--
Th	2.53	1.76	5.72	7.14	4.78	0.69	6.58	1.15	4.78	5.79	1.36	1.52	1.07	3.28	3.88	2.92	3.05	2.06
U	0.67	0.53	1.28	1.92	1.37	<3.86	1.80	<0.8	1.20	1.80	<0.7	<0.6	<0.8	1.12	0.98	<0.9	<0.8	--

TABLE 1: Major and trace element contents of the phonolites and trachytes from Axum, northern Ethiopia. Data from Hagos et al. (2010). All major element and trace element contents of: V, Ni, Cu, Ga, Sr, Y, Zr and Nb were determined using the XRF spectrometry, and the contents of remaining trace elements and all rare earth elements were determined using INAA at the Department of Lithospheric Sciences, University of Vienna. Total Fe as Fe_2O_3.

mately one kilogram of sample material for crushing and preparation of powders for chemical analyses. Petrographic thin-sections were also prepared for 32 samples from each of the basaltic, trachytic and phonolitic rocks, and detailed mineralogical analyses were made under an optical (petrographic) microscope. For some of the minerals, the semiquantitative volume estimates were determined by visually estimating the mineral proportions in thin sections.

From the 33 analyzed samples 19 were from the two types of basalts and the remaining samples were from the phonolitic - trachytic rocks of the Bete-Giorgis, Gobo-Dura, Adi-Tsehafi, and Mai-Koho ridges. All rock samples were first crushed in a stainless steel jaw crusher and then powdered in an agate mill in order to avoid contamination of transition elements (such as Co, Ta, and Nb) for the chemical analyses. Contents of major oxides, minor and trace element (Nb, Zr, Y, Sr, Ga, Cu, Ni, V) abundances were determined using wavelength-dispersive XRF spectrometry at the Department of Lithospheric Research, University of Vienna, Austria. 1.2 g of powdered rock was mixed with 6 g of lithium tetra-borate to prepare fused pellets used for the analyses of the major oxides, and 10 g of powdered rock was used to prepare pressed pellets for the analyses of the trace elements.

Contents of the rare earth element (REE) and other trace elements (i.e., Sc, Cr, Co, Zn, As, Se, Br, Rb, Sb, Cs, Ba, Hf, Ta, W, Ir, Au, Th, and U) were analyzed by INAA at the Department of Lithospheric Research, University of Vienna. For this, samples weighing between 115 and 130 mg were sealed into polyethylene capsules, as well as 60- to 100 mg of three of the following international rock standards: carbonaceous chondrite Allende (Smithsonian Institute, Washington DC, USA; Jarosewich et al., 1987), the granite AC-E (Centre de Recherche Pétrographique et Géochimique, Nancy, France: Govindaraju, 1989), and the Devonian Ohio shale SDO-1 (United States Geological Survey, Govindaraju, 1989) were irradiated for 8 hours at the Triga Mark II reactor of the Atominstitut der Österreichischen Universitäten, Vienna, at a neutron flux of 2.10^{12} n cm^{-2} s^{-1}. Details of the INAA method, including standards, correction procedures, precision, and accuracy, are reported in Koeberl (1993), Son and Koeberl (2005), and Mader and Koeberl (2010).

4.2. Results

4.2.1 Major elements

According to the total alkali-silica (TAS) classification of Le Bas et al. (1986) (Fig. 4) the volcanic rocks of the Axum – Shire area belong to phonolites, trachytes, basaltic-trachyandesites, basalts, trachybasalts, basanites, and tephrites show a range in the SiO$_2$ contents from 43 to 69 wt% (Table 1). The Axum volcanic rocks plot in the alkaline field or slightly within the transition field, with the exception of one sample (AX12). All basaltic rocks have <49 wt% SiO$_2$ contents and high (~4.3 – 7.4 wt%) Na$_2$O + K$_2$O contents. The phonolitic–trachytic rocks of the area have 58 – 69 wt% SiO$_2$ contents. The Bete-Giorgis phonolites are silica-undersaturated (58.6 – 59.3 SiO$_2$ wt%), with very high Al$_2$O$_3$ (18.5 – 19 wt%) and Na$_2$O (8.9 – 9.9 wt%) contents. The CIPW normative compositions of the Axum volcanics (Table 2) reflect these geochemical variations. All samples from the Axum volcanic rocks, except the samples from the Mai-Koho trachytes, are normative quartz-free (Table 2). The Mai-Koho trachytes (silica-oversaturated) contain a significant amount of normative quartz (5 – 9.5 wt%). All rocks of the post-trap basalt sequence and some of the flood basalt sequence are basanites and/or alkali-olivine basalts. However, an olivine tholeiite tendency is observed for the flood basalt sequence group (e.g., AX12, AX29, and AX32).

The alkali contents of the Gobo-

Axum alkaline basalts
▲ Post-trap basalt Sequence
■ Flood basalt Sequence
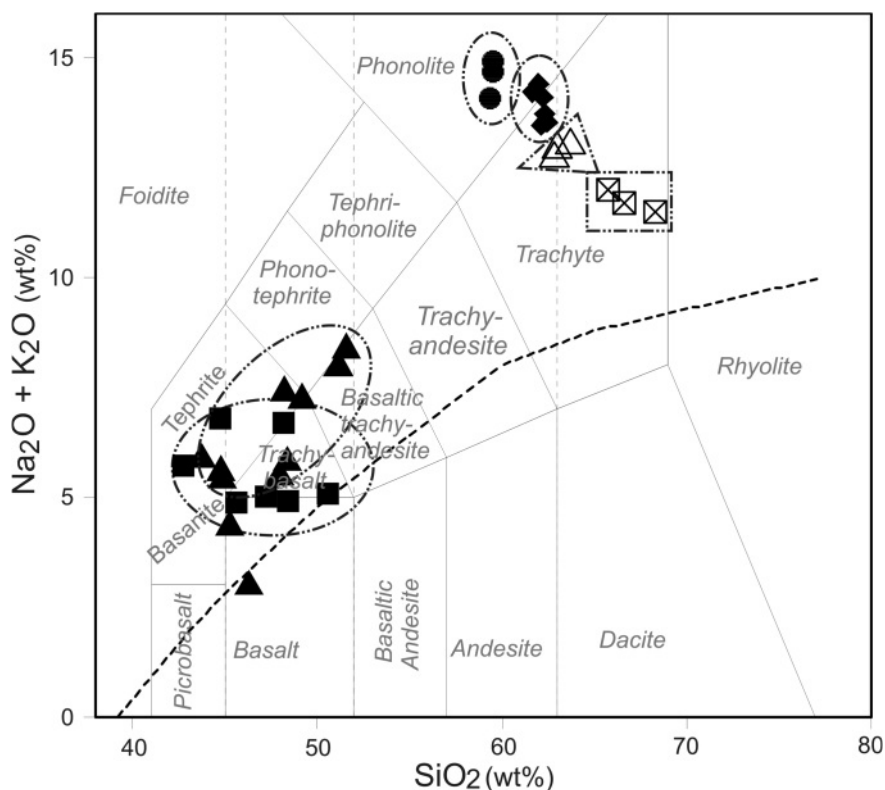
Acidic rocks
● Bete-Giorgis phonolites   △ Adi-Tsehafi trachytes
◆ Gobo-Dura phonolites   ⊠ Mai-Koho trachytes

FIGURE 4: Total alkali-silica diagram comparing the geochemical characteristics of the volcanic rocks of Axum. The dashed line distinguishes tholeiitic from alkaline basalts (from Le Bas et al., 1986).

Dura phonolites vary between 13.4 and 14.5 wt % $Na_2O + K_2O$. Samples AX11, 12 and 45 correspond to the Bete-Giorgis phonolites; whereas samples AX06, 10a and 45c are analogous to the foid-bearing trachytes (the Adi-Tsehafi trachytes). The Adi-Tsehafi trachytes, on the other hand, do not show a wide range in alkalinity; however, all samples plot close to the phonolite-trachyte boundary (Fig. 4). The compositions of the felsic rocks from Axum, therefore, correlate linearly in the TAS diagram and their total alkali ($Na_2O + K_2O$) contents or their alkalinities decrease systematically from the Bete-Giorgis phonolite to the Mai-Koho trachytes, whereas the SiO_2 (wt%) contents increase (Fig. 4).

Almost all basalt samples, except sample AX47b, are highly to moderately fractionated mafic rocks with MgO values between 2 and 8 wt% (Hagos et al., 2010). The distribution of TiO_2 in the basaltic, tephritic, and basanitic rocks of the area covers a wide range (1.5 – 4.4 wt%) and shows two well-defined trends: the low-Ti post-trap basalt sequence and the high-Ti flood basalt sequence (Fig. 5a). The MgO and TiO_2 contents in the phonolite – trachyte rocks are very low (0.01 – 0.14 wt% MgO and 0.03 – 0.15 wt% TiO_2). Instead, the content of Al_2O_3 is very high (16.5 – 19 wt%), which exceeds the contents of $Na_2O + K_2O + CaO$ and follows the same trend as that for the total alkalis (Fig. 5c). Generally, the Axum phonolitic – trachytic rocks have very low but nearly identical contents of TiO_2, MgO, and CaO. The Al_2O_3, Na_2O, K_2O, and MnO contents are very high (Fig. 5a – h). Most of the samples from the Bete-Giorgis and Gobo-Dura phonolites have significant Cl contents (0.12 – 0.34 wt%), in contrast to the low contents in the basalts and trachytes of the region.

4.2.2 Trace elements

The trace element contents of the Axum basaltic sequences are highly variable. The post-trap basalt sequence displays the highest incompatible trace element contents. In contrast, the flood basalt sequence is less enriched. This is illustrated in Figs. 6b, d, e, and h, where selected trace element contents are plotted against SiO_2 contents. Negative correlations in the plots of the contents of some incompatible trace elements vs. SiO_2 (wt%) are observed in the basaltic sequences (Fig. 6a and f) and the alkaline acidic rocks (Fig. 6b, d and e) of Axum. Negative correlations are also observed for the V and Ni vs. SiO_2 contents (not plotted). The contents of incompatible trace elements, such as Nb, Zr, and the REE, increase with the silica content up to the phonolitic-trachytes (Adi-Tsehafi trachytes), but are slightly lower again in the Mai-Koho trachytes. The content of Y increases slightly from the basanites to the basaltic trachy-andesites, shows very high values in the Bete-Giorgis phonolites, and decreases sharply from the Gobo-Dura phonolites to the Mai-Koho trachytes.

The chondrite-normalized REE patterns for the post-trap basalts and the flood basalt sequence are different (Fig. 7a). The post-trap basalt sequence has highly sloping light REE (LREE) and relatively flat heavy REE (HREE) patterns; in contrast

SAMPLE	Rock Name	Qz	or	ab	an	ne	di	hy	ol	ac	mt	il	ap	nms
AX43	Phonolite		28.9	37.5		17.8	4.1		2.6	7.9		0.1	0.1	0.8
AX111	Phonolite		30.3	37.0		16.9	6.4		1.5	5.9	1.0	0.1	0.1	
AX112	Phonolite		28.5	37.3		16.9	3.6		2.8	7.9		0.1	0.1	1.4
AX011	Phonolite		28.5	49.5		8.4	2.7		2.6	7.0		0.1	0.1	1.2
AX012	Phonolite		30.1	47.5		8.6	3.7		2.4	7.4		0.1	0.1	0.2
AX45	Phonolite		28.5	48.2		9.1	2.5		2.8	7.0		0.1	0.1	1.9
AX45C	Phonolite		30.4	48.1		8.4	3.5		2.3	7.0		0.1	0.1	0.2
AX06	Phonolite		28.5	37.3		17.0	3.6		2.8	7.9		0.1	0.1	1.4
AX10a	Phonolite		32.6	45.4		7.2	4.2		2.5	7.2	0.4	0.1	0.1	
AX41	Trachyte		28.0	53.9		6.2	2.7		2.9	5.1		0.1	0.1	0.3
AX07	Trachyte		31.1	50.9		3.5	3.3		4.0	6.0	0.4	0.2	0.1	
AX10b	Trachyte		31.5	50.8		3.0	5.2		2.8	4.7	1.1	0.2	0.1	
AX002	Trachyte	6.5	30.1	55.9	0.4		2.4	2.0			2.4	0.3	0.1	
AX008	Trachyte	9.4	29.1	56.0	1.5		0.3	2.4			1.6	0.1	0.1	
AX51	Trachyte	5.0	31.8	55.6	0.4	0.6	3.3				2.5	0.3	0.1	
AX004	Basalt		9.4	16.8	14.5	10.0	15.2		19.3		5.0	8.3	2.2	
AX09	Basalt		8.1	28.7	21.8	0.3	7.8		18.5		4.8	7.5	1.4	
AX29	Basalt		6.2	32.8	21.3		8.6	9.5	9.1		4.5	6.7	1.2	
AX32	Basalt		6.6	32.7	24.4		5.4	1.1	17.5		4.3	6.2	1.1	
AX42	Basalt	1.4	10.3	28.4	24.1		5.4	19.4			3.9	5.5	1.9	
AX44	Basalt		3.4	41.3	16.3	4.9	2.7		17.6		4.6	5.4	1.4	
AX63	Basalt		8.7	24.4	10.4	11.7	15.8		12.9		7.6	5.8	3.0	
AX20	Basalt		10.1	6.0	18.7	15.7	24.0		15.0		3.8	4.9	1.6	
AX21	Basalt		6.6	14.1	17.6	12.4	21.6		15.6		3.7	5.6	1.8	
AX24	Basalt		11.4	21.4	19.8	6.6	19.0		15.2		3.1	4.0	1.3	
AX31	Basalt		12.3	25.2	22.5	10.7	9.6		10.8		3.2	4.0	1.9	
AX34	Basalt		10.9	21.4	21.5	5.3	17.4		16.3		3.2	4.3	1.2	
AX38	Basalt		6.2	11.2	20.2	13.6	26.4		11.4		3.4	4.6	2.0	
AX43D	Basalt		5.7	39.7	14.9	6.9	5.4		16.8		4.2	4.2	1.6	
AX47B	Basalt		9.0	10.9	22.5	7.2	21.8		20.9		3.4	4.1	1.3	

Table 2: CIPW norm calculation in wt% for the volcanic rock of Axum, northern Ethiopia. The norm calculation was from the CIPW software. Qz: quartz; or: orthoclase; ab: albite; an: anorthite; ne: nepheline; di: diopside; hy: hypersthenes; ol: olivine; ac: acmite; mt: magnetite; il: ilmenite; ap: apatite; nms: metasilcate. The Fe^{2+}/Fe^{3+} ratios for basalts, trachytes and phonolites are 4:1, 3:2 and 1:1 respectively.

the flood basalt sequence has a comparatively flat LREE and moderately slopping HREE pattern. The average chondrite-normalized La/Yb ratios (13.1) of the post-trap basalt sequence are higher than the value for flood basalt sequence, which is

7.7 (Hagos et al., 2010).

Chondrite-normalized incompatible trace element diagrams (Fig. 7b) show generally a coherent behavior with enriched low-field strength elements (Ba, Rb, K) and depleted high-field
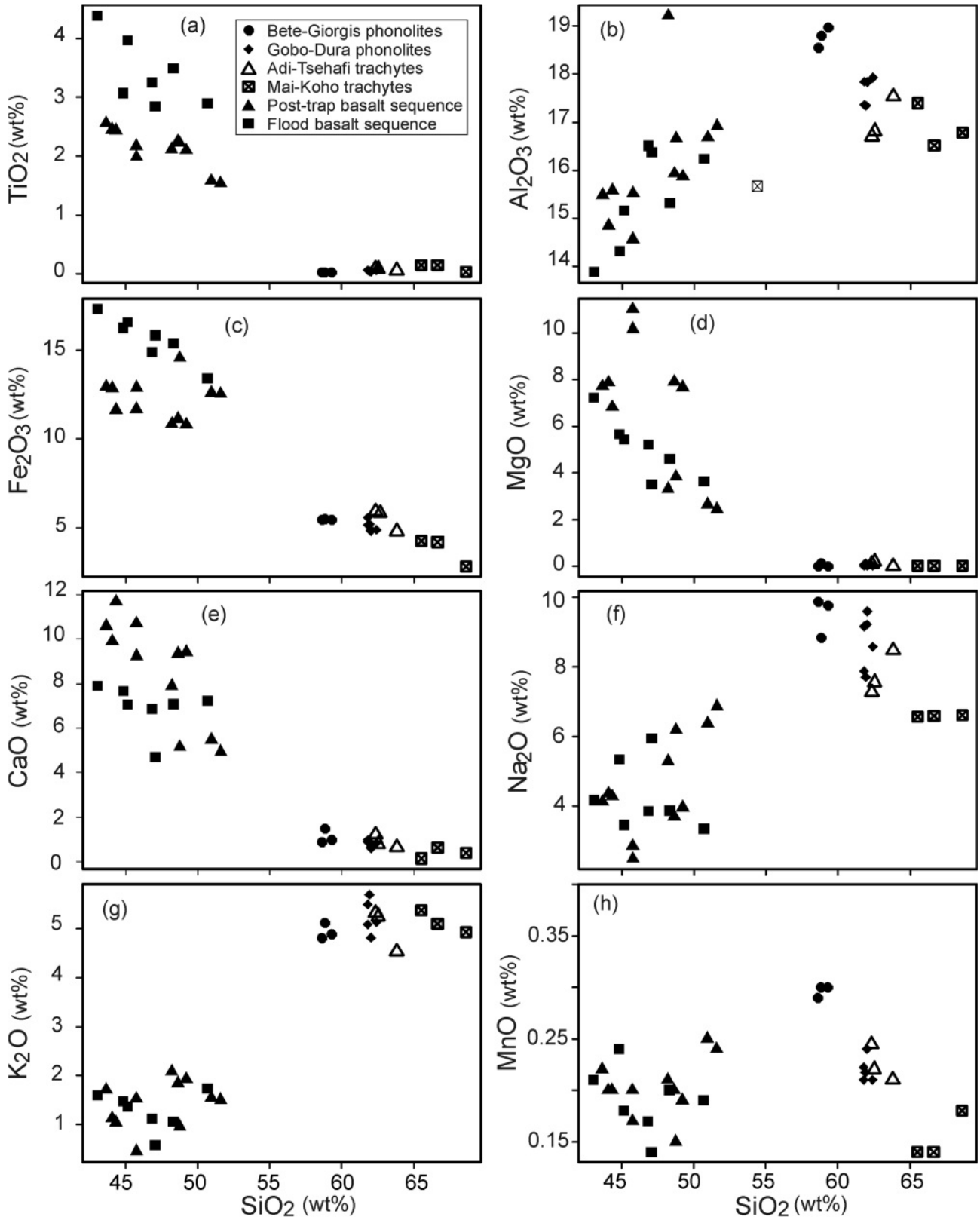

Figure 5: Harker variation diagrams for the bimodal volcanic rocks of Axum area. All the major oxides are characterized by their unique trend as SiO2 progress from 43 – 69 wt%.

strength elements (Zr, Hf, Y) throughout the post-trap basalt sequence; however, this behavior is reversed for the flood

basalt sequence. In the normalized multi-element diagram the elemental contents of Nb and Ta in the post-trap basalt se-
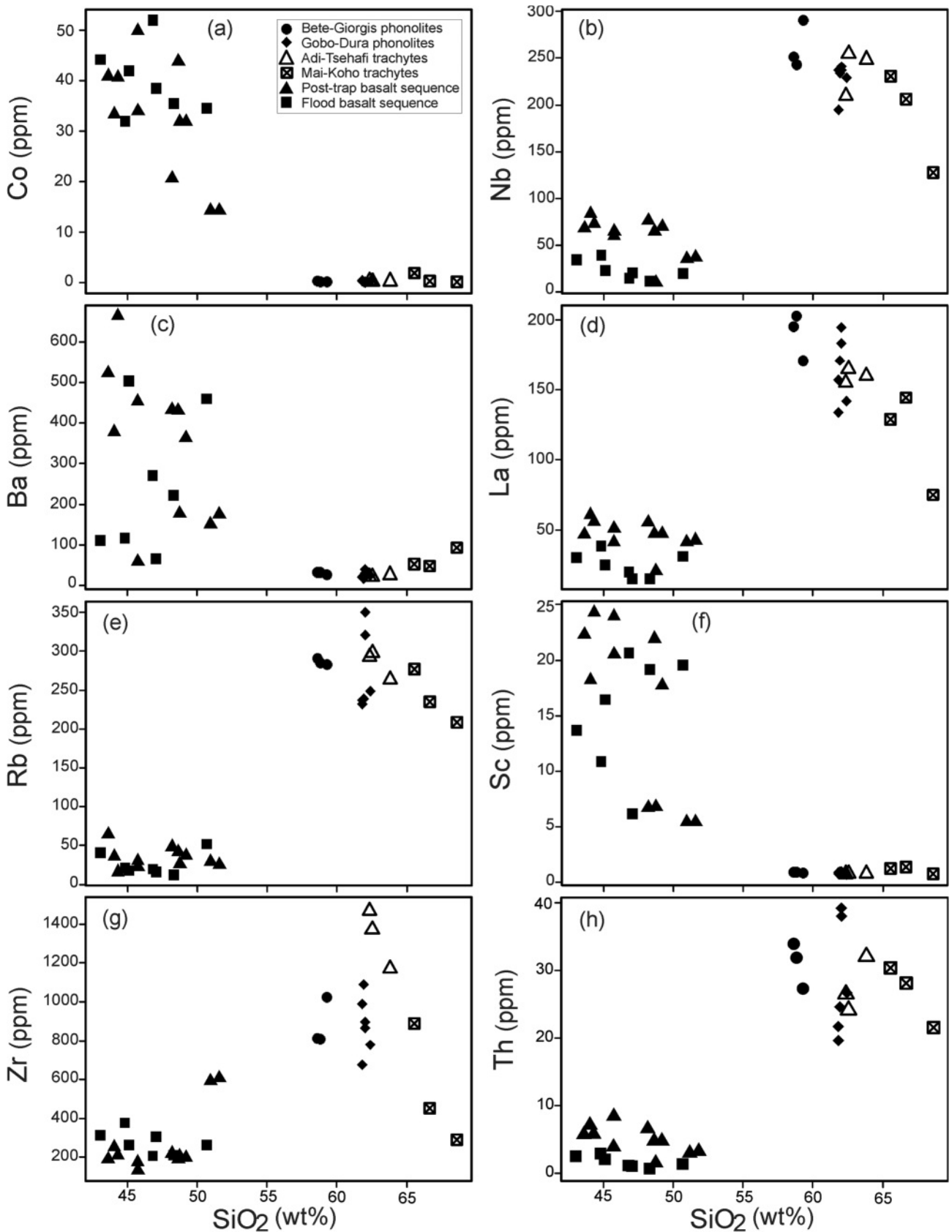
FIGURE 6: Plots of selected trace element contents (ppm) against differentiation index (SiO2 wt%) for the Axum volcanic rocks. The binary plots of the contents of Sc, Co, Rb, Th, Zr, Nb, Ba, and La versus SiO2 illustrate the compositional variation among the Axum volcanic rocks.

quence are enriched by a factor of 3 compared to the flood basalt sequence, but the Sr, Nd, and Yb concentrations in both rocks are similar (Hagos et al., 2010).

The phonolite - trachyte rocks have similar chondrite-normalized REE patterns. All have steep LREE and flat HREE patterns. They also show strong negative Eu anomalies with (Eu/Eu*)$_n$ ratios ranging from 0.21 to 0.30 for the Bete-Giorgis and Gobo-Dura phonolites and 0.12 to 0.33 for the Adi-Tsehafi and Mai-Koho trachytes (Table 1). The trachytes have a wider range of the (Eu/Eu*)$_n$ ratio and this shows that there is a relatively broader compositional range than for the phonolites.

5. Discussion

The volcanic rocks of the northern Ethiopia in general, and the Axum volcanic rocks in particular, are among the least studied parts of the Ethiopian flood basalts. The Axum volcanics

are highly diversified and cover the range from basanites/tephrites, basalts, trachybasalts, and basaltic trachy-andesites to phonolites and trachytes. Hagos et al. (2010) conducted a geochemical study on the Axum volcanics and found two groups (post-trap basalt and flood basalt sequences) of mildly to highly alkaline basaltic rocks.

5.1 The alkaline basalts of Axum

Pik et al. (1998, 1999) grouped the Axum volcanics as transitional to tholeiitic low-Ti basalts, but our study on the northern end of the Ethiopian flood basalt confirmed that the Axum volcanic rocks are not tholeiitic in character; instead they are alkaline constituting a wide range in the TiO$_2$ content and highly diversified rocks (trachybasalts – basanites – tephrites) (Fig. 4).

Based on the TiO$_2$ content and the incompatible trace element concentration variations, the Axum basalts are grouped
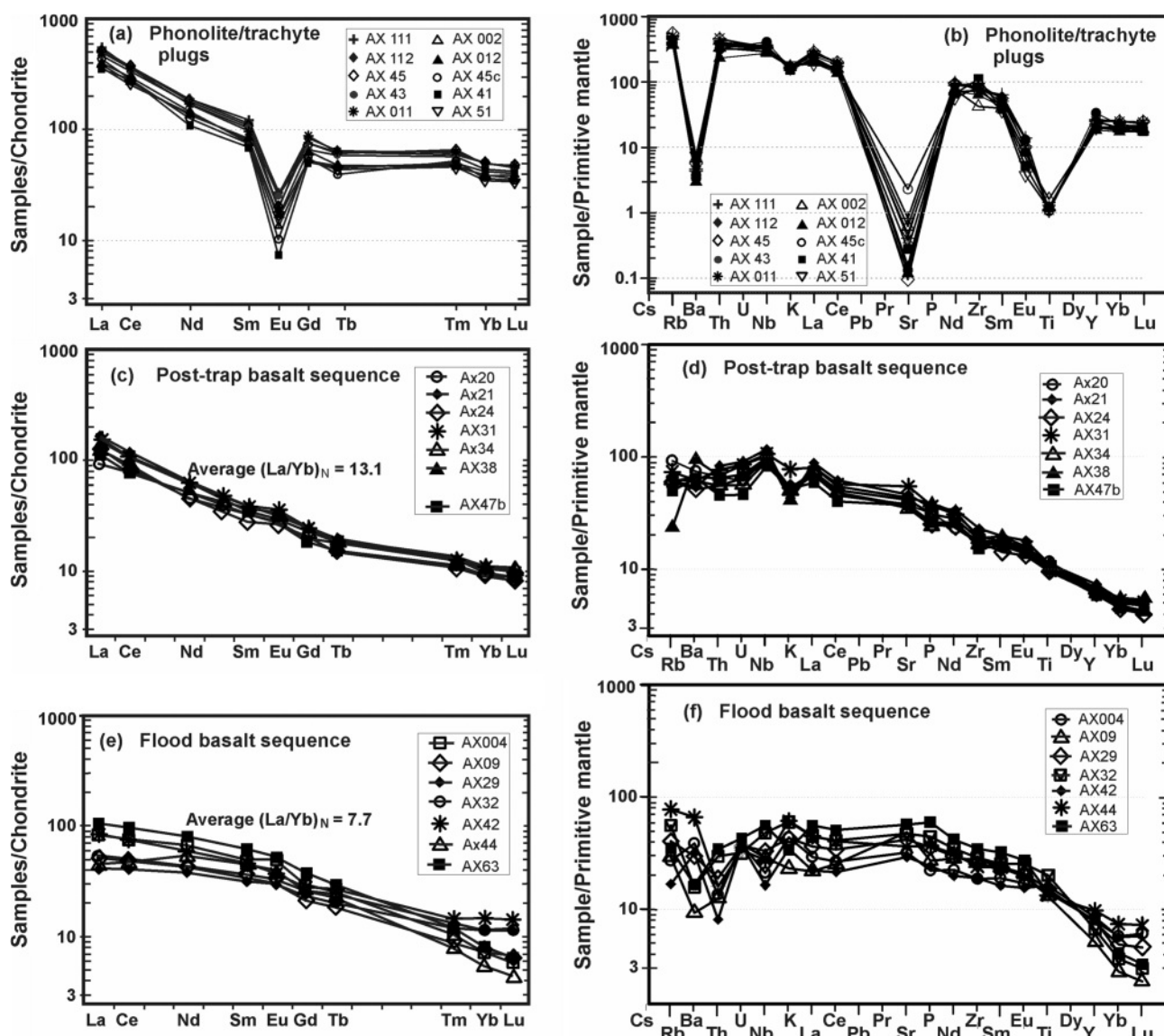
Figure 7: Chondrite-normalized rare earth and primitive mantle-normalized incompatible trace element abundance patterns of the Axum volcanic rocks. Normalization factors after Taylor and McLennan (1985) for the chondrite-normalization, and Sun and McDonough (1989) for the primitive mantle normalization. (a) steeply inclined light REE, strong negative Eu anomaly and gently inclined heavy REE. (b) strong negative anomalies are observed at Ba, Sr, and Ti.

in to two parts as post-trap basalt sequence (1.5 – 2.6 TiO$_2$ wt%) and flood basalt sequence (2.6 – 4.5 TiO$_2$ wt%) (Hagos et al., 2010). The different elemental compositions of post-trap basalt and flood basalt sequences are clearly evident on TiO$_2$ vs. SiO$_2$, Nb vs. La, Hf vs. Th, Nb/Y vs. Zr, and La/Sm vs. Gd/Yb plots (Fig. 8). The rocks from the post-trap basalt sequence, with their unique geochemical signature, are unlike those in any other part of the Ethiopian flood basalt province (Fig.8); however, Zanettin et al. (1999, 2006b) and Kieffer et al. (2004) documented the existence of low-Ti alkali basalts in the central Eritrean highlands (Adi Ugri and Asmara basalts) and in the central part of the northwestern Ethiopian volcanic province (Choke and Guguftu shield volcanoes), respectively. Zanettin et al. (2006a) believed that during the early Miocene (24 – 22 Myr) this alkaline magmatism extended from Adi Ugri (Mendefera), and perhaps also from Adwa-Axum to Senafe. Kieffer et al. (2004) also confirmed that the Choke and Guguftu shield volcanoes erupted around 22 Ma ago contemporaneously with the central Eritrean Alkali basalts.

The post-trap basalt sequence is fresh, unaltered, undefor-
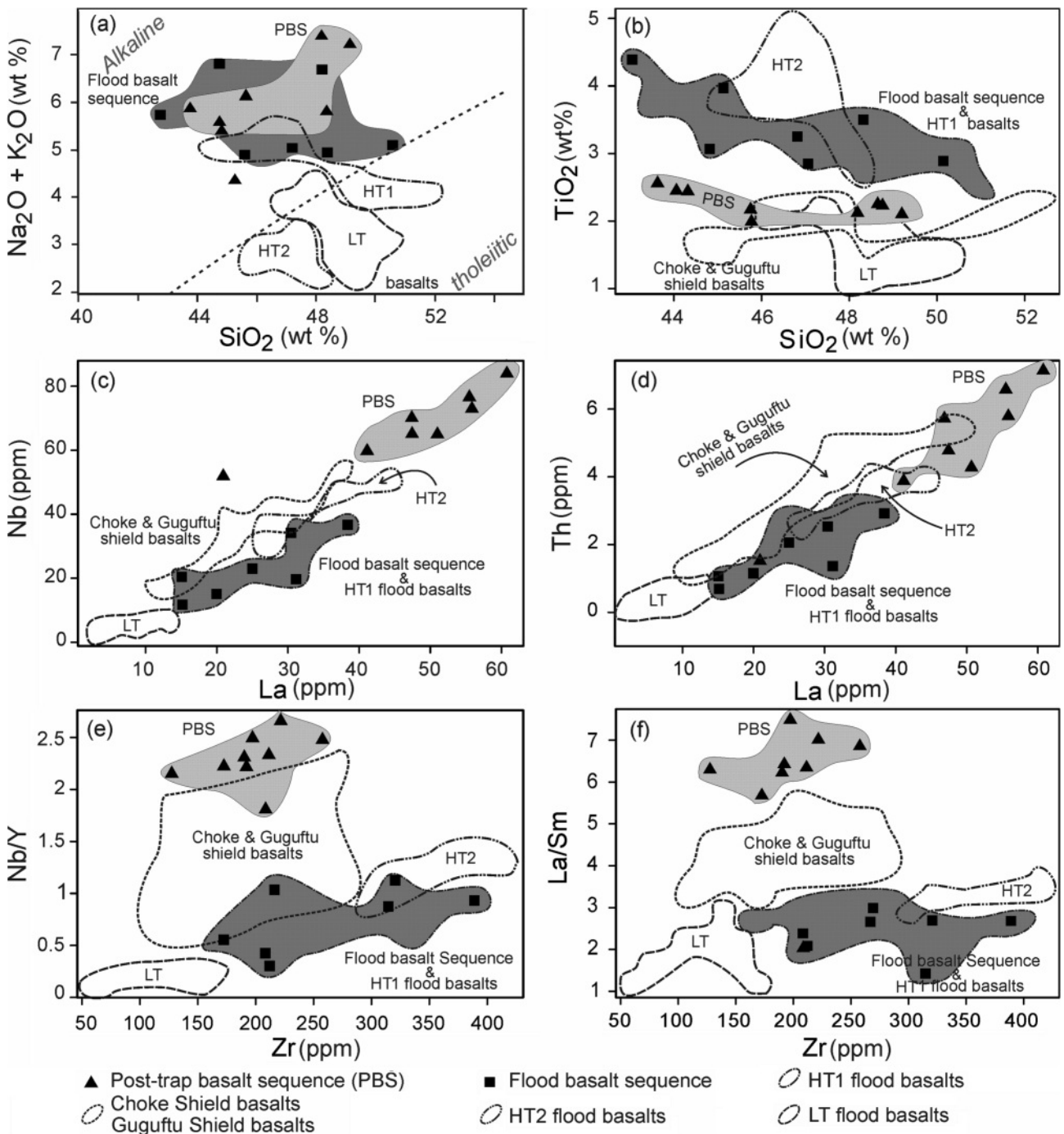
FIGURE 8: Binary plots of major element, trace element, and ratio comparing the Axum alkaline basalts with the northwestern Ethiopian flood basalts and shield volcanoes; (a and b) major oxides vs. SiO$_2$ (wt %); (c and d) highly incompatible trace elements (Nb and Th) vs. La, and (e and f) ratios of the important trace elements (Nb/Y and La/sm) vs. Zr contents.

med and overlies a deeply and newly eroded basement complex, indicating the relatively young time of emplacement of these basalts. Several authors confirmed that the post-trap alkaline rocks span a wide time of eruption. The silica-undersaturated rock types (basanites, nephelinites, and phonolites) in some of the younger shield volcanoes are even younger (25 to 5 Ma; Zanettin et al., 1976). Kieffer et al. (2004) have also pointed out that the post-trap magmatism in the Ethiopian highland is getting younger north or southwards of the Choke and Guguftu shield basalts. Mt. Guna, which erupted to the north of the Choke and Guguftu shields, has an Ar/Ar age of 10.7 Ma (Kieffer et al., 2004 and references therein). Although the absence of geochronological data constrains the study of temporal relationship of Axum post-trap basalt sequence with the other post-trap basaltic rocks of Ethiopia, our geochemical analyses of rocks from the Axum area reveal that there is a similarity with the composition of the Guguftu shield volcano (Fig. 8b, d, e, and f). In several binary element plots the post-trap basalt sequence of Axum is tightly clustered, with very high contents of Nb, La, Th, Ta, and high Nb/Y and La/Sm ratios. In contrast, the composition of the Guguftu shield basalt is less tightly clustered and has moderate to high contents of Nb, La, Th, as well as moderate Nb/Y and La/Sm ratios. These

alkaline post-trap basalts of Axum display extremely high incompatible trace element contents that are characteristic of magmas formed by low degrees of partial melting, most probably during the last phase of the Ethiopian plateau volcanism.

The Axum flood basalt sequence shows broad geochemical characteristics ranging from highly to mildly alkaline basaltic suites. This flood basalt does not share any geochemical characteristics with the Axum post-trap basalt sequence, except their alkalinity (Fig. 8a-f). Instead, our geochemical data of the flood basalt sequence from the Axum area complement the Adigrat data (samples E215 and E217) reported by Pik et al. (1998, 1999).

Figure 8 shows that in terms of their trace element contents and ratios, the flood basalt sequence from the Axum area resemble Pik et al.'s (1999) HT1 flood basalt from the Adigrat area. Both basalts share an alkaline – mildly alkaline magmatic character with relatively moderate concentrations of the highly incompatible trace elements and moderately fractionated trace element patterns. In most of the binary plots (Fig. 8b, c, e, and f) both basaltic suites cluster in the same region and it is difficult to differentiate them. The trends observed in Figure 8, and the strongly differentiated nature of these lavas, suggest that their characteristics could result from upper crus-
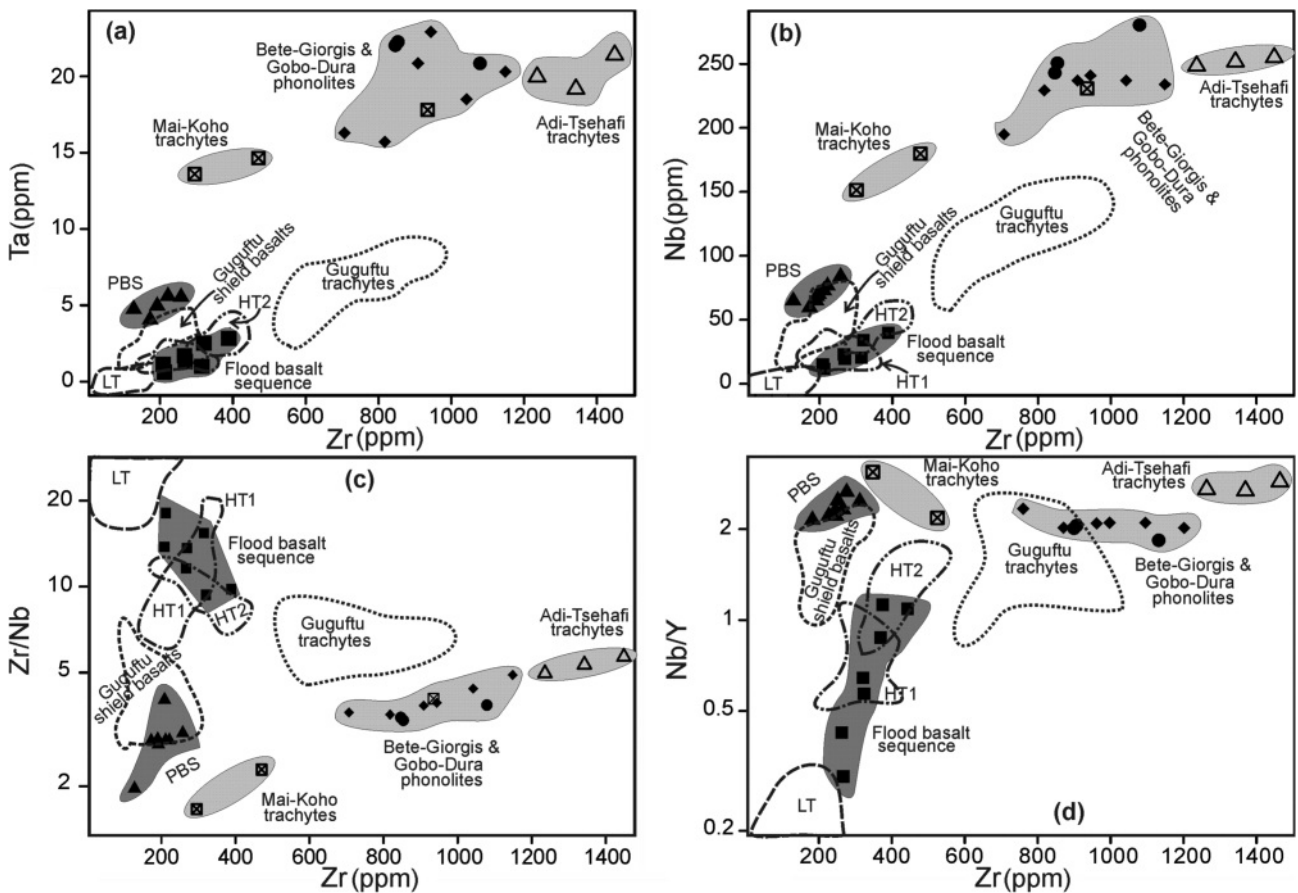

FIGURE 9: (a and b) Plots of Ta vs. Zr and Nb vs. Zr, showing the two apparent evolution trends for the Axum volcanics and the other Ethiopian flood basalts and shield volcanoes. Most Axum flood basalt sequence and the other Ethiopian volcanics rocks plot at lower Ta and Nb contents. (c) Zr/Nb vs Zr plot for the volcanic rocks. The post-trap basalt sequence with their cogenetic acidic rocks have the same low Zr/Nb ratio, however, the flood basalt sequence and other Ethiopian volcanics rocks have a higher and wider Zr/Nb ratio. (d) Nb/Y vs. Zr plot showing high Nb/Y ratios for the post-trap basalt sequence with their co-genetic acidic rocks.

tal contamination of mantle-derived magmas (Pik et al., 1999).

5.2 The Axum Miocene- to Pliocene phonolite – trachyte plugs

There is no reliable evidence whether or not the Axum phonolite–trachyte plugs are coeval with the Ethiopian shield volcanoes or if they are Pliocene- to recent alkaline acidic rocks that extruded/intruded the trap along the ENE trending northern Afar lineament. It is evident from the field observation that the Axum phonolites and trachytes do not interfinger with the Axum flood basalt sequence, but instead they are overlying these basalts and, at places, intrude and deform the basaltic flow layers. There, the phonolitic/trachytic domes reach their maximum frequency and dimension, and overlie the schistose basement, Mesozoic sandstone, and trap volcanic rocks. According to Zanettin et al. (2006b and references therein) the "domiform lavas" were erupted after a long erosive cycle, in the course of which both the Magdala stratoid volcanic rocks and the sandstone were locally removed, thus uncovering the basement schists. These authors hypothesized that the age of the domes was rather recent, Quaternary or Late Pliocene, and assigned the same age to the acid domes in the Senafe area.

The silica-poor rocks at Axum constitute the Bete-Giorgis phonolites, the Gobo-Dura trachy-phonolites, and the Adi-Tsehafi phonolitic trachytes. Each of these rock types has distinct geochemical and petrographic characteristics. However, their trace element ratios (e.g., Zr/Nb, Nb/Y, La/Lu) show limited variation, which indicates a homogeneous source region. Geochemically, these alkaline rocks, including the peralkaline trachytes, correspond to the silicic rocks of the central and southeastern Eritrea (Zanettin et al., 2006b), which are characterized by very low contents of MgO (0.02 – 0.2 wt%); however, the Eritrean silicic rocks cover relatively diversified suites, from tephri-phonolite to rhyolite. The Axum acidic rocks, on the other hand, are less diverse, ranging from phonolites to trachytes, and

exhibit gradual variation from the nepheline-rich to the nepheline-poor rocks.

5.3 The alkaline basalt – phonolitic/trachytic magma interactions of the Axum volcanic rocks.

The post-trap and flood basalt sequences of the Axum area exhibit major petrogenetic differences (Hagos et al., 2010). The accompanying phonolites and trachytes correspond to the incompatible element-enriched post-trap basalt sequence. The petrogenetic relationship between the basalts and the phonolite/trachyte rocks is inferred from binary and ternary plots of the contents of incompatible trace elements and their ratios (Figs. 9 and 10). The Zr vs. Ta and Zr vs. Nb diagrams show a well-defined linear correlation among the post-trap basalt sequence and the phonolitic/trachytic rocks (Fig. 9a and b), and their incompatible element abundances progressively increase with increasing degree of fractionation. Similarity of incompatible trace element is often cited as strong evidence that fractional crystallization has been the dominant process in the evolution of mafic to felsic magmatic suites (Weaver 1977; Wilson, 1995). The Zr/Nb ratio of the Axum phonolites and trachytes and the post-trap basalt sequence is nearly constant (Fig. 9c; 3 – 4.5) with the exception of the Adi-Tsehafi trachytes, which have relatively higher Zr/Nb ratios ranging from 5 – 5.7, which are still much lower than in the Axum flood basalt (Zr/Nb 10 – 18; Fig. 9c).

Low Nb/La ratios (<1.0) in volcanic rocks are a reliable trace element index of crustal contamination (Kieffer et al., 2004). The tholeiitic basalts of the Ethiopian flood volcanics have persistently low Nb/La ratios, typical of crustal contamination, whereas alkali basalts from the late veneer on the Simien shield, samples from all other shields, and the HT1 and HT2 lavas of Pik et al. (1999), have high Nb/La ratios (Kieffer et al., 2004). Our data support this interpretation. The same behavior is seen in the Axum volcanics, where a persistent crus-
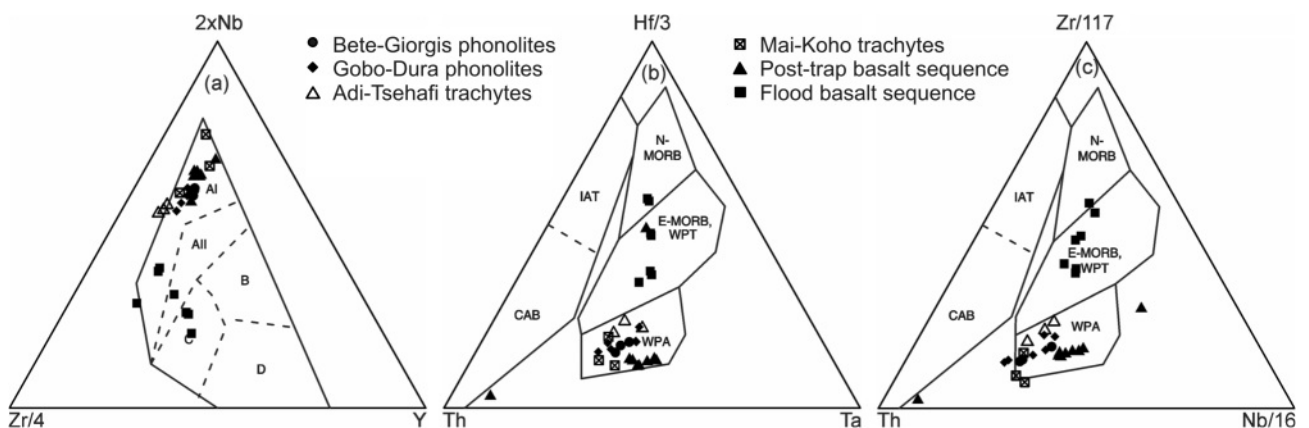

FIGURE 10: Discrimination diagrams, showing that the Axum volcanic rocks plot into two clusters in all the three diagrams: (a) The Zr-Nb-Y discrimination diagram for the Axum basalts and phonolites. Volcanic rocks from various tectonic provinces generally fall into these fields: AI–AII: within-plate alkali basalts; AII-C: within-plate tholeiitic basalts; B: P-type mid-oceanic ridge basalts; D: N-type mid-oceanic ridge basalts; C-D: volcanic arc basalts (Meschede, 1986). (b) The Th-Hf-Ta discrimination diagram divides the triangle into; N-MORB: normal-type mid-oceanic ridge basalt; E-MORB (WPT): enriched mid-oceanic ridge basalt (with-in-plate tholeiite; WPA: within-plate alkali; and IAT; island-arc tholeiite (Wood, 1980). (c) The Th-Zr-Nb discrimination diagram also divides the triangle into: N-MORB, E-MORB (WPT), WPA, and IAT (Wood, 1980).

tal signature is absent in the alkaline volcanic rocks.

The Zr/Nb ratios in volcanic rocks may also reflect crustal contamination or variation in degree of partial melting (Wilson et al., 1995; Kamber and Collerson, 2000). The Adi-Tsehafi trachyte is sandwiched between the Chila granite and the Mesozoic sandstone unit. The slight increase in the Zr/Nb ratio for the Adi-Tsehafi trachyte reflects relatively low degree of partial melting or crustal involvement either from the sandstone or late Proterozoic Chila granite.

At given Zr contents most of the post-trap basalt sequence samples have higher Ta, Nb, and Th contents and Nb/Y ratio (Fig. 9a, b and d) than do the flood basalt sequence. Kamber and Collerson (2000) have indicated that Nb is more sensitive to variations in degrees of partial melting than Zr, and hence can be used to constrain the influence of variable degrees of melting. The discrimination diagrams Zr/4-2xNb-Y, Th-Hf/3-Ta, and Th-Zr/117-Nb/16 of Axum volcanic rocks form two clusters (Fig. 10a-c). The samples from the Axum flood basalt sequence fall within the enriched-MORB of within-plate basalts, and the samples from the post-trap basalt sequence and the phonolites/trachytes of Axum indistinguishably plot within the within-plate alkali basalt field. Hagos et al. (2010) stated that the source reservoirs for both the post-trap and the flood basalt sequences seems to be one and the same and resembles those of the OIB, but the main petrogenetic change between these two basaltic rocks of Axum would be most probably in the degree and mechanism of partial melting of the rocks in the mantle plume.

6. Conclusions

All possible combinations of the REE, trace element contents and their ratios confirmed that the Axum area experienced two volcanic episodes. The first volcanic episode, the Axum flood basalt sequence, occurred contemporaneously with the northwestern Ethiopian flood basalts. The second magmatic episode, the Axum post-trap basalt sequence and associated felsic rocks, evolved most probably during the last phase of the Ethiopian shield basalts. From the geochemical analyses, the flood basalt sequence of Axum and the HT1 flood basalts of Adigrat are indistinguishable. However, the second group of basalts, the post-trap basalt sequence, exhibits different and distinct geochemical characteristics.

Unlike the alkaline basalts, the phonolites and trachytes of Axum exhibit similar geochemical characteristics. The contents of oxides (Al_2O_3, Fe_2O_3, Na_2O, MnO) and the trace elements (Nb, La, Rb, Zr) decrease linearly with increasing SiO_2 content from the Bete-Giorgis phonolites to the Mai-Koho trachytes. All these rocks have a similar degree of fractionation that is characterized by very low MgO and TiO_2 contents, ranging from 0.01 – 0.14 wt% and 0.03 – 0.15 wt%, respectively.

The Nb vs. Zr, Zr/Nb vs. Zr, and Nb/Y vs. Zr binary plots and the Zr/4-2xNb-Y, Th-Hf/3-Ta, and Th-Zr/117-Nb/16 discrimination diagrams confirmed that the post-trap basalt sequence, the phonolites, and the trachytes evolved from the same parental magma that invaded some parts of the west-central Ti-

gray and most probably the central and southeastern part of Eritrea (Adi-Ugri, Asmara, and Senafe volcanic rocks) ~19 to 6 Ma after the major Ethiopian flood basalts.

References

Alemu, T., 1998. Geochemistry of Neoproterozoic granitoids from the Axum Area, northern Ethiopia. Journal of African Earth Sciences, 27, 437–460.

Alene, M., Secco, L., Dal Negro, A. and Sacchi, R., 2000. Crystal chemistry of clinopyroxene in Neoproterozoic metavolcanic rocks of Tigrai, Northern Ethiopia. Bollettino della Societa Geologica Italiana, 119, 581 – 586.

Asrat, A., Gleizes, G., Barbey, P. And Ayalew, D., 2003. Magma emplacement and mafic - felsic magma hybridisation: structural evidence from the Pan-African Negash pluton, Northern Ethiopia. Journal of Structural Geology, 25, 1451–1469.

Asrat, A., Barbey, P., Ludden, N.J., Reisberg, L., Gleizes, G. and Ayalew, D., 2004. Petrology and isotope geochemistry of the Pan-African Negash pluton, northern Ethiopia: Mafic-Felsic magma interactions during the construction of shallow-level calc-alkaline plutons. Journal of Petrology, 45, 1147–1179.

Ayalew, D., Yirgu, G. and Pik, R., 1999. Geochemical and isotopic (Sr, Nd and Pb) characteristics of volcanic rocks from south-western Ethiopia. Journal of African Earth Sciences, 29, 381–391.

Ayalew, D., Barbey, P., Marty, B., Reisberg, L., Yirgu, G. and Pik R., 2002. Source, genesis and timing of giant ignimbrite deposits associated with Ethiopian continental flood basalts. Geochimica et Cosmochimica Acta, 66, 1429–1448.

Baker, J., Snee, L. and Menzies, M., 1996. A brief Oligocene period of flood volcanism in Yemen: implications for the duration and rate of continental flood volcanism at the Afro-Arabian triple junction. Earth and Planetary Science Letters, 138, 39–55.

Barrat, J.A., Fourcade, S., Jahn, B.M., Chemirke, J.L. and Capdevila, R., 1998. Isotope (Sr, Nd, Pb, O) and trace-element geochemistry of volcanics from the Erta' Ale range (Ethiopia). Journal of Volcanology and Geothermal Research, 80, 85–100.

Berhe, S. M., Desta, B., Nicoletti, M. and Teferra M., 1987. Geology, geochronology and geodynamic implications of the Cenozoic magmatic province in W and SE Ethiopia. Journal of the Geological Society, London, 144, 213–226.

Beyth, M., 1972. The geology of central and western Tigray. Ph.D thesis, Rheinische Friedrich-Wilhelms Universität, Bonn, W. Germany, 200 pp.

Dainelli, G., 1943. Geologia dell' Africa orientale. Regia Accademia d'Italia Centro studi per l' Africa oriental Italiana, Rome, Italy, 1–4.

Ebinger, C. J. and Sleep, N.H., 1998. Cenozoic magmatism throughout East Africa resulting from impact of a single plume. Nature, 395, 788–791.

Ethiopian Institute of Geological Survey, 1999. Aksum map sheet ND 37-6 (scale 1:250,000), Geological Survey of Ethiopia, Addis Ababa, Ethiopia.

Furman, T., Bryce, G.J., Karson, J. and Lotti, A., 2004. East African rift system (EARS) plume structure: Insights from Quaternary mafic lavas of Turkana, Kenya. Journal of Petrology, 45, 1069–1088.

George, R.M., Rogers, N. and Kelley, S., 1998. Earliest magmatism in Ethiopia: Evidence for two mantle plumes in one flood basalt province. Geology, 26, 923–926.

Govindaraju. K.. 1989. 1989 combilation of working values and sample description for 272 geostandards. Geostandards Newsletter, 13, 1–113.

Hagos, M., Koeberl, C., Kabeto, K. and Koller, F., 2010. Geology, petrology and geochemistry of the basaltic rocks of the Axum area, northern Ethiopia. In: J. Ray, G. Sen, B. Ghosh (eds.) Topics in Igneous Petrology: A Tribute to Prof. Mihir K. Bose, Springer, Heidelberg , in press.

Hofmann, C., Courtillot, V., Feraud, G., Rochette, P., Yirgu, G., Ketefo, E. and Pik, R., 1997. Timing of the Ethiopian flood basalt event and implications for plume birth and environmental change. Nature, 389, 838–841.

Jarosewich, E., Clarke, R.S.J. and Barrows, J.N., 1987. The Allende meteorite reference sample. Smithsonian Contributions to Earth Sciences, 27, 1–49.

Kabeto, K., Sawada, Y., Bussert, R. and Kuster, D., 2004. Geology and geochemistry of Mai-chew volcanics, northwestern Ethiopian Plateau. International Conference on East African Rift system, Addis Ababa, Ethiopia. Extended Abstract, 1, 110–114.

Kamber, B.S. and Collerson, K.D., 2000. Zr/Nb systematics of ocean island basalts reassessed - The case for binary mixing. Journal of Petrology, 41, 1007–1021.

Kieffer, B., Arndt, N., Lapierre, H., Bastien, F., Bosch, D., Pecher, A., Yirgu, G., Ayalew, D., Weis, D., Jerram, A.D., Keller, F. and Meugniot, C., 2004. Flood and shield basalts from Ethiopia: magmas from the African superswell. Journal of Petrology, 45, 793–834.

Koeberl, C., 1993. Instrumental neutron activation analysis of geochemical and cosmochemical samples: A fast and reliable method for small sample analysis. Journal of Radioanalytical and Nuclear Chemistry, 168, 47–60.

Kuster, D., Dwivedi, S.B., Kabeto, K., Mehary, K. and Matheis, G., 2005. Petrogenetic reconnaissance investigation of mafic sills associated with flood basalts, Mekelle basin, northern Ethiopia: implication for Ni-Cu exploration. Journal of Geochemical Exploration, 85, 63–79.

Le Bas, M.L., Le Maitre, R.W., Streckeisen, A. and Zanettin, B., 1986. A chemical classification of volcanic rocks based on the total alkali – silica diagram. Journal of Petrology, 27, 745 – 750.

Mader, D. and Koeberl, C., 2009. Using instrumental neutron activation analysis for geochemical analyses of terrestrial impact structures: Current analytical procedures at the laboratory. Applied Radiation and Isotopes, 67, 2100–2103.

Meschede, M., 1986. A method of discriminating between different types of mid-oceanic ridge basalts and continental tholeiites with the Nb-Zr-Y diagram. Chemical Geology, 56, 207–218.

Mohr, P., 1983. Ethiopian flood basalt province. Nature, 303, 577–584.

Pik, R., Deniel, C., Coulon, C., Yirgu, G., Hoffmann, C. and Ayalew, D., 1998. The northwestern Ethiopian Plateau flood basalts: classification and spatial distribution of magma types. Journal of Volcanology and Geothermal Research, 81, 91–111.

Pik, R., Deniel, C., Coulon, C., Yirgu, G. and Marty, B., 1999. Isotopic and trace element signatures of Ethiopian basalts: evidence for plume-lithospheric interactions. Geochimica et Cosmochimica Acta, 63, 2263–2279.

Stewart, K. and Rogers, N., 1996. Mantle plume and lithosphere contributions to basalts from Southern Ethiopia. Earth and Planetary Science Letters, 139, 195–211.

Son, T.H. and Koeberl, C., 2005. Chemical variations within fragments of Australasian tektites. Meteoritics and Planetary Science, 40, 805–815.

Sun, S. and McDonough, W.F., 1989. Chemical and isotopic systematics of oceanic basalts: implications for mantle composition and processes. In Saunders, A.D. and Norry, M.J. (Eds.) Magmatism in the ocean basins. Geological Society London, Special Publication, 42, 313–345.

Tadesse, T., 1996. Structure across a possible intra-oceanic suture zone in the low-grade Pan-African rocks of northern Ethiopia. Journal of African Earth Sciences, 23, 375–381.

Tadesse, T., 1997. The Geology of Axum area (ND 37-6). Memoir no. 9, Ethiopia Institute of Geological Survey, Addis Ababa, Ethiopia, 184 pp.

Taylor, S.R. and McLennan, S.M., 1985. The continental crust: Its composition and evolution. Blackwell, Oxford, 312 pp.

Ukstins, I., Renne, P., Wolfenden, E., Baker, J., Ayalew, D. and Menzies, M., 2002. Matching conjugate volcanic rifted margins: $^{40}Ar/^{39}Ar$ chronostratigraphy of pre- and syn-rift bimodal flood volcanism in Ethiopia and Yemen. Earth and Planetary Science Letters, 198, 289–306.

Weaver, S.D., 1977. The Quaternary Caldera Volcano Emuruangogolak, Kenya Rift, and the Petrology of a Bimodal Ferrobasalt-Pantelleritic-Trachyte Association. Bulletin of Volcanology, 40, 209–230.

Wilson, M., Downes, H. and Cebriá, J., 1995. Contrasting fractionation trends in coexisting continental alkaline magma series; Cantal, Massif Central, France. Journal of Petrology, 36, 1729 –1753.

Wood, D.A., 1980. The application of a Th-Hf-Ta diagram to problems of tectono-magmatic classification and to establishing the nature of crustal contamination of basaltic lavas of the British Tertiary volcanic province. Earth and Planetary Science Letters, 50, 11–30.

Zanettin, B., Bellieni, G., Visentin, J.E. and Haile, T., 1999. The volcanic rocks of the Eritrean plateau: stratigraphy and evolution. Acta Volcanologica, 11, 183–193.

Zanettin, B., Bellieni, G. and Visentin, J.E., 2006a. New radiometric age of volcanic rocks in the Central Eritrean plateau (from Asmara to Adi Quala): considerations on stratigraphy and correlations. Journal of African Earth Science, 45, 156–161.

Zanettin, B., Bellieni, G. and Visentin, J.E., 2006b. Stratigraphy and evolution of the trachy – rhyolitic volcanism of the Senafe area (eastern Eritrean plateau). Journal of African Earth Sciences, 45, 478–488.

Miruts HAGOS[1)*)], Christian KOEBERL[1)], Kurkura KABETO[2)] & Friedrich KOLLER[1)]

[1)] Department of Lithospheric Research, University of Vienna, Althanstrasse 14, A-1090 Vienna, Austria;

[2)] Department of Earth Sciences, Mekelle University, Mekelle, Ethiopia;

[*)] Corresponding author, miruts2005@yahoo.com